



# Measurement of the local and nonlocal amplitudes in $B^+ \rightarrow K^+ \mu^+ \mu^-$ decays

LHCb collaboration<sup>†</sup>

## Abstract

This paper presents a thorough study of the local and nonlocal amplitudes in  $B^+ \rightarrow K^+ \mu^+ \mu^-$  transitions through an amplitude analysis of the dimuon mass spectrum of the decay. The analysis is based on  $pp$  collision data corresponding to an integrated luminosity of  $8.4 \text{ fb}^{-1}$  collected by the LHCb experiment. This measurement employs a model that describes both one-particle and two-particle nonlocal amplitudes across the entirety of the dimuon mass spectrum, enabling the determination of both short- and long-distance contributions to the decay. The compatibility of the Wilson coefficient combinations  $C_9 + C'_9$  and  $C_{10} + C'_{10}$  with the Standard Model prediction is found to vary between  $1.6 \sigma$  and  $4 \sigma$ , depending on the choice of local form factors.

Submitted to JHEP

© 2026 CERN for the benefit of the LHCb collaboration. [CC BY 4.0 licence](#).

<sup>†</sup>Authors are listed at the end of this paper.



# 1 Introduction

Over the past decade, a broad set of measurements of  $b \rightarrow s\mu^+\mu^-$  transitions has revealed a consistent pattern of tensions with Standard Model (SM) predictions, attracting considerable interest from both the theoretical and experimental communities [1, 2]. In this context, the decay  $B^+ \rightarrow K^+\mu^+\mu^-$  plays a central role as it is both experimentally and theoretically simpler compared to other  $b \rightarrow s\mu^+\mu^-$  transitions, since only a single charged pseudoscalar hadron is present in the final state.<sup>1</sup> This paper presents a model-dependent analysis of the long- and short-distance contributions in  $B^+ \rightarrow K^+\mu^+\mu^-$  decays across the reconstructed dimuon mass range  $300 < m_{\mu\mu} < 4700 \text{ MeV}/c^2$  using a data sample corresponding to an integrated luminosity of  $8.4 \text{ fb}^{-1}$  of  $pp$  collisions collected during Run 1 and Run 2 of the LHCb experiment. The measurements presented here supersede those in Ref. [3] by employing a more complete description of the long-distance amplitudes and including Run 2 data.

The  $b \rightarrow s\ell^+\ell^-$  transitions are studied in the framework of weak effective theories where the dimension-six effective Hamiltonian is defined as a sum of operators ( $\mathcal{O}_i$ ) with Wilson coefficients  $C_i$ ,

$$\mathcal{H}^{\text{eff}} = -\frac{4G_F}{\sqrt{2}}V_{tb}V_{ts}^* \sum_i C_i^{(\prime)}(\mu)\mathcal{O}_i^{(\prime)}(\mu), \quad (1)$$

where  $G_F$  is the Fermi constant,  $V_{tq}^{(*)}$  are the Cabibbo–Kobayashi–Maskawa (CKM) matrix elements, and  $\mu$  defines the energy scale. The Wilson coefficients,  $C_i^{(\prime)}$ , encode the heavy short-distance physics, while the operators,  $\mathcal{O}_i^{(\prime)}$ , account for the long-distance contributions. By measuring the Wilson coefficients, the presence of short-distance new physics can be established.

The local contributions to the decay rate correspond to the SM electroweak penguin contribution and new-physics amplitudes, which mediate the decay. The nonlocal contributions are generated through four-quark operators that interact electromagnetically with a  $\mu^+\mu^-$  pair. As described in Ref. [4], these nonlocal amplitudes can be modelled through the sum of one-particle (1p)  $J^{PC} = 1^{--}$  charmonium and light-quark states, and two-particle (2p) amplitudes comprising  $B^+ \rightarrow K^+(D^{(*)}\bar{D}^{(*)} \rightarrow \mu^+\mu^-)$  processes, where  $D^{(*)}$  denotes a ground-state or excited charm meson.

Global analyses of differential branching fraction measurements and angular distributions of  $B^+ \rightarrow K^+\mu^+\mu^-$ ,  $B^0 \rightarrow K^*(892)^0\mu^+\mu^-$  and other  $b \rightarrow s\mu^+\mu^-$  decays performed in bins of the squared invariant mass of the dimuon system ( $q^2$ ), exhibit tensions with SM predictions [5–15] consistent with the presence of new physics in the Wilson coefficient  $C_9$ . However, there is considerable debate regarding the possibility of underestimated nonlocal contributions in the SM predictions of  $b \rightarrow s\mu^+\mu^-$  observables that can mimic new physics [16–27].

Recently, the LHCb collaboration performed amplitude analyses of the  $B^0 \rightarrow K^*(892)^0\mu^+\mu^-$  decay using different models to describe the nonlocal amplitude across the decay phase space [28, 29]. These measurements resulted in a data-driven determination of the dominant hadronic contributions while confirming the tension in  $C_9$ , albeit with reduced statistical precision.

---

<sup>1</sup>The inclusion of charge-conjugate processes is implied throughout, unless otherwise specified.

The paper is structured as follows: a detailed description of the nonlocal model is given in Sec. 2. In Sec. 3 the LHCb detector and simulation procedure are introduced, and in Sec. 4 the candidate selection procedure is discussed. The selection efficiency, resolution and background models are discussed in Sec. 5, followed by a description of the sources of systematic uncertainty and the method adopted to account for them in Sec. 6. The fit to the dimuon spectrum and the systematic effects are presented and the results discussed in Sec. 7, followed by the conclusion in Sec. 8.

## 2 Differential decay rate

Following the model described in Ref. [4], the  $CP$ -averaged differential decay rate of  $B^+ \rightarrow K^+ \mu^+ \mu^-$  decays is given by

$$\begin{aligned} \frac{d\Gamma_\mu}{dq^2} = & \frac{G_F^2 \alpha^2 |V_{tb} V_{ts}^*|^2}{128\pi^5} |\mathbf{k}| \beta_+ \left\{ \frac{2}{3} |\mathbf{k}|^2 \beta_+^2 |C_A f_+(q^2)|^2 + \frac{m_\mu^2 (M_B^2 - M_K^2)^2}{q^2 M_B^2} |C_A f_0(q^2)|^2 \right. \\ & \left. + |\mathbf{k}|^2 \left[ 1 - \frac{1}{3} \beta_+^2 \right] \left| C_V f_+(q^2) + 2(C_7^{\text{eff}} + C_7') \frac{m_b + m_s}{M_B + M_K} f_T(q^2) \right|^2 \right\}, \end{aligned} \quad (2)$$

where  $M_K$  and  $M_B$  are the masses of the kaon and  $B$  meson,  $m_b$ ,  $m_s$  and  $m_\mu$  are the masses of the  $b$  quark,  $s$  quark and the muon, respectively. The factor  $|\mathbf{k}|$  is the magnitude of the kaon momentum in the rest frame of the  $B$  meson and  $\beta_+^2 \equiv 1 - 4m_\mu^2/q^2$ . The parameter  $\alpha$  is the QED fine structure constant. The parameters  $f_{0,+T}$  are the scalar, vector and tensor  $B \rightarrow K$  form factors. This analysis employs lattice QCD computations for these quantities.

The Wilson coefficients  $C_{V,A}$  are defined as  $C_{V,A} \equiv C_{9,10} + C'_{9,10}$ , where  $C_9$ ,  $C_{10}$  correspond to the coupling strength of the vector and axial-vector current operators  $\mathcal{O}_9$  and  $\mathcal{O}_{10}$ . The Wilson coefficients  $C'_9$ ,  $C'_{10}$  correspond to the right-handed counterparts of operators  $\mathcal{O}'_9$  and  $\mathcal{O}'_{10}$ . The dependence of Eq. 2 on  $C_{V,A}$  makes a fit to the differential decay rate of  $B^+ \rightarrow K^+ \mu^+ \mu^-$  transitions unable to distinguish between the left- and right-handed counterparts of  $C_9$  and  $C_{10}$ . For the measurements presented in this paper,  $C_7^{\text{eff}}$  is set to the SM value given in Ref. [13],  $C_7'$  is set to zero, and all Wilson coefficients are assumed to be real. The values of all the constants used in Eq. 2 are summarised in Table 1.

The  $q^2$ -dependent nonlocal amplitudes are included in the decay rate through the redefinition of

$$C_9 \rightarrow C_9^{\text{eff}} \equiv C_9 + Y_{\text{light}}^{1\text{p}}(q^2) + Y_{c\bar{c}}^{1\text{p}+2\text{p}}(q^2), \quad (3)$$

where  $Y_{\text{light}}^{1\text{p}}$  and  $Y_{c\bar{c}}^{1\text{p}+2\text{p}}$  are the total amplitudes of the light one-particle states and the sum of one-particle and two-particle  $c\bar{c}$  states, respectively. Following Ref. [4], the functions  $Y_{\text{light}}^{1\text{p}}$  and  $Y_{c\bar{c}}^{1\text{p}+2\text{p}}$  are written in terms of hadronic dispersion relations.

The one- and two-particle  $c\bar{c}$  amplitudes are given by the following expression

$$Y_{c\bar{c}}^{1\text{p}+2\text{p}}(q^2) = Y_{c\bar{c}}^0(q_0^2) + \Delta Y_{c\bar{c}}^{1\text{p}}(q^2) + \Delta Y_{c\bar{c}}^{2\text{p}}(q^2), \quad (4)$$

with  $Y_{c\bar{c}}^0(q_0^2)$  representing the subtraction constant of the dispersion relation. In this analysis, the subtraction point is chosen to be  $q_0^2 = 0$ , following Ref. [13], with

Table 1: The values for the constants used in the measurement presented in this paper, taken from Refs. [13, 30].

Constant	Value
$G_F$	$1.1745 \times 10^{-5} \text{ GeV}^{-2}$
$ V_{tb} V_{ts}^* $	0.04185
$M_B$	5279.26 MeV/ $c^2$
$M_K$	493.677 MeV/ $c^2$
$m_b$	4870 MeV/ $c^2$
$m_s$	95 MeV/ $c^2$
$m_\mu$	105.658 MeV/ $c^2$
$C_7^{\text{eff}}$	-0.450
$\alpha(m_b)$	1/133

$Y_{c\bar{c}}^0(0) = 0.230 \pm 0.065$ . The one-particle  $c\bar{c}$  contribution is modelled as

$$\Delta Y_{c\bar{c}}^{1\text{p}}(q^2) = \sum_j \eta_j e^{i\delta_j} \frac{(q^2 - q_0^2)}{(m_j^2 - q_0^2)} A_j^{\text{res}}(q^2), \quad (5)$$

where  $\eta_j$  and  $\delta_j$  are the magnitude and phase of the  $j^{\text{th}}$  resonant contribution relative to the local  $B^+ \rightarrow K^+ \mu^+ \mu^-$  amplitude. For the  $J/\psi$ ,  $\psi(2S)$ ,  $\psi(4040)$ ,  $\psi(4160)$  and  $\psi(4415)$  resonances, the factor  $A_j^{\text{res}}(q^2)$  is given by a relativistic Breit–Wigner function as shown below

$$A_j^{\text{res}}(q^2) = \frac{m_j \Gamma_{0j}}{(m_j^2 - q^2) - im_j \Gamma_j(q^2)}, \quad (6)$$

where  $m_j$  and  $\Gamma_{0j}$  represent the mass and natural width of the resonance and the running width  $\Gamma_j(q^2)$  is given by

$$\Gamma_j(q^2) = \frac{p(m_\mu, q^2)}{p(m_\mu, m_j^2)} \frac{m_j}{\sqrt{q^2}} \Gamma_{0j}, \quad (7)$$

with

$$p(m, x) = \frac{\sqrt{x}}{2} \sqrt{1 - \frac{4m^2}{x}}. \quad (8)$$

For the  $\psi(3770)$  resonance  $A_j^{\text{res}}(q^2)$  takes the form of a Flatté function [31] to account for the open-charm threshold at  $2m_D$ . Therefore, in this case, the running width of the  $\psi(3770)$  state is given by

$$\Gamma_j(q^2) = \frac{p(m_\mu, q^2)}{p(m_\mu, m_j^2)} \frac{m_j}{\sqrt{q^2}} \Gamma_{\psi(3770),1} + \frac{p(m_D, q^2)}{p(m_D, m_j^2)} \frac{m_j}{\sqrt{q^2}} \Gamma_{\psi(3770),2}. \quad (9)$$

The two widths  $\Gamma_{\psi(3770),1}$  and  $\Gamma_{\psi(3770),2}$  are taken from Ref. [30] and correspond to the partial widths of  $\psi(3770)$  decaying to final states below and above the open-charm threshold. The two-particle charm contributions are given by,

$$\Delta Y_{c\bar{c}}^{2\text{p}}(q^2) = \sum_j \eta_{2\text{p}}^j e^{i\delta_{2\text{p}}^j} A_j^{2\text{p}}(q^2) \quad (10)$$

with

$$A_j^{2p}(q^2) = \frac{(q^2 - q_0^2)}{\pi} \int_{q_{min}^2}^{\infty} ds \frac{\hat{\rho}_j(s)}{(s - q_0^2)(s - q^2 - i\epsilon)}, \quad (11)$$

where the sum in Eq. 10 runs over the  $D\bar{D}$ ,  $D\bar{D}^*$  and  $D^*\bar{D}^*$  contributions, and the normalised spectral densities of the two-particle states are modelled by the two-body phase space  $\hat{\rho}_j$ . The lower threshold of the integral  $q_{min}^2$  is taken to be just below the  $D\bar{D}$  threshold. The parameters  $\eta_{2p}^j$  and  $\delta_{2p}^j$  are the magnitude and phase of each of the two-particle states and are measured from data. Following the approach of Ref. [4], the conservation of angular momentum and parity in the two-particle production dictate that the two-particle states are produced in a P-wave configuration. In this case, the integral in Eq. 11 can be approximated to give

$$\Delta Y_{c\bar{c}}^{2p}(q^2) = \eta_{2p} e^{i\delta_{2p}} \sum_j h_P(m_j, q^2) \quad (12)$$

with

$$h_P(m, q^2) = \frac{2}{3} + \left(1 - \frac{4m^2}{q^2}\right) h_S(m, q^2), \quad h_S(m, q^2) = 2 - G\left(1 - \frac{4m^2}{q^2}\right), \quad (13)$$

where

$$G(y) = \sqrt{|y|} \left\{ \Theta(y) \left[ \ln \left( \frac{1 + \sqrt{y}}{1 - \sqrt{y}} \right) - i\pi \right] + 2 \Theta(-y) \arctan \left( \frac{1}{\sqrt{-y}} \right) \right\}. \quad (14)$$

The similarity in the  $q^2$  dependence of the  $D\bar{D}$ ,  $D\bar{D}^*$  and  $D^*\bar{D}^*$  amplitudes means that the  $D\bar{D}$ ,  $D\bar{D}^*$  and  $D^*\bar{D}^*$  two-particle contributions can be effectively approximated with a single term with magnitude  $\eta_{2p}$  and phase  $\delta_{2p}$ . This assumption is necessary to ensure fit stability given the data sample size used in this analysis.

As presented in Ref. [4], the two-particle model adopted in this paper allows for the inclusion of a  $B^+ \rightarrow K^+(\tau^+\tau^- \rightarrow \mu^+\mu^-)$  nonlocal amplitude whose magnitude is quantified through the lepton-flavour-universality-violating Wilson coefficient  $C_{9\tau}$ . However, the approximation of having a single magnitude and phase to describe all three  $D\bar{D}$ ,  $D\bar{D}^*$  and  $D^*\bar{D}^*$  amplitudes results in a large systematic uncertainty on a measurement of  $C_{9\tau}$ . As such, more data are required to enable the determination of  $C_{9\tau}$  without relying on a simplified treatment of the two-particle charm rescattering amplitudes.

A procedure analogous to that used for the  $c\bar{c}$  contributions is adopted for the light-quark nonlocal amplitudes. In this case, an unsubtracted dispersion relation is employed, and the contribution from the light-quark 2p amplitudes is omitted, in line with Ref. [4]. The resulting light-quark nonlocal contribution is given by

$$Y_{\text{light}}^{1p}(q^2) = \sum_j \eta_j e^{i\delta_j} A_j^{\text{res}}(q^2), \quad (15)$$

where the sum runs over the  $\rho(770)$ ,  $\omega(782)$  and  $\phi(1020)$  states. In this case,  $A_j^{\text{res}}(q^2)$  is given by a relativistic Breit–Wigner function shown in Eq. 6, while the  $\phi(1020)$  amplitude,  $A_j^{\text{res}}(q^2)$  takes the form defined in Ref. [32] that accounts for the open-kaon threshold.

The  $q^2$ -dependent width of the  $\phi(1020)$  amplitude is given by

$$\begin{aligned}\Gamma_{\phi(1020)}(q^2) &= \left( \frac{p(m_{K^+}, q^2)}{p(m_{K^+}, m_{\phi(1020)}^2)} \right)^3 \frac{m_{\phi(1020)}}{\sqrt{q^2}} \Gamma_{\phi(1020) \rightarrow K^+ K^-} \\ &+ \left( \frac{p(m_{K^0}, q^2)}{p(m_{K^0}, m_{\phi(1020)}^2)} \right)^3 \frac{m_{\phi(1020)}}{\sqrt{q^2}} \Gamma_{\phi(1020) \rightarrow K^0 \bar{K}^0} \\ &+ \left( \Gamma_{\phi(1020)} - \Gamma_{\phi(1020) \rightarrow K^+ K^-} - \Gamma_{\phi(1020) \rightarrow K^0 \bar{K}^0} \right),\end{aligned}\quad (16)$$

where  $p(m_l, x)$  is given in Eq. 8,  $\Gamma_{\phi(1020)}$  represents the full decay width of the  $\phi(1020)$  state and  $\Gamma_{\phi(1020) \rightarrow K^+ K^-}$ ,  $\Gamma_{\phi(1020) \rightarrow K^0 \bar{K}^0}$  correspond to the given partial widths. The mass and width of the  $\phi(1020)$  meson are taken from Ref. [33].

The branching fraction of the nonlocal states,  $\mathcal{B}(B^+ \rightarrow K^+ X_j) \times \mathcal{B}(X_j \rightarrow \mu^+ \mu^-)$ , is given by,

$$\frac{\tau_B G_F^2 \alpha^2 |V_{tb} V_{ts}^*|^2}{\hbar 128 \pi^5} |\eta_j|^2 \int_{4m_\mu^2}^{(m_B - m_K)^2} |\mathbf{k}|^3 \left[ \beta_+ - \frac{1}{3} \beta_+^3 \right] |f_+(q^2)|^2 |S_j(q^2) A_j^{\text{res}}(q^2)|^2 dq^2, \quad (17)$$

where  $\tau_B$  is the  $B^+$ -meson lifetime, and  $\hbar$  is the reduced Planck's constant. The factor  $S_j(q^2) = \frac{q^2}{m_j^2}$  for the charmonium resonances and  $S_j(q^2) = 1$  for the light resonances. The branching fractions of intermediate 2p states can be calculated by making the substitution  $A_j^{\text{res}} \rightarrow A_j^{2p}$  and using  $S_j(q^2) = 1$ .

The parameters of interest in this analysis are the Wilson coefficients  $C_V$  and  $C_A$ , and the magnitudes and phases ( $\eta_i$ ,  $\delta_i$ ) of the nonlocal amplitudes. The effect of  $CP$  violation has been found to be small across the  $m_{\mu\mu}$  range [34], including the region around the  $\rho(770)$  and  $\omega(782)$  resonances, whose contributions carry an SM weak phase [35]. As a consequence, this analysis is currently not sensitive to  $CP$ -violating effects at low dimuon masses. Therefore,  $\eta_i$  and  $\delta_i$  are taken to be the same for  $B^+$  and  $B^-$  decays throughout.

The magnitudes and phases of all the charmonium resonances are measured from data except for the  $J/\psi$  state. The  $J/\psi$  resonance is used as the normalisation channel and therefore its magnitude is fixed while the phase is measured relative to the local amplitude. In Ref. [4] the spectral densities of the 2p states are written using two-body Källén functions at their respective thresholds. Based on this, the approximate solution to the 2p amplitudes is used in this analysis.

Two separate computations of the local  $B \rightarrow K$  form factors are employed in this analysis. The baseline implementation uses the parametrisation and form-factor results of the High Precision Lattice QCD (HPQCD) collaboration [36], with those of the Fermilab and MIMD Lattice Computation (FNAL/MILC) collaboration [37] used as a cross-check. In both cases, all form-factor parameters are allowed to vary in the fit to the data, subject to constraints from their respective determinations in Refs. [36, 37].

### 3 Detector and simulations

The LHCb detector [38, 39] is a single-arm forward spectrometer covering the pseudorapidity range  $2 < \eta < 5$ , designed for the study of particles containing  $b$  or

$c$  quarks. The detector used to collect the data analysed in this paper includes a high-precision tracking system consisting of a silicon-strip vertex detector surrounding the  $pp$  interaction region [39], a large-area silicon-strip detector located upstream of a dipole magnet with a bending power of about 4 T m, and three stations of silicon-strip detectors and straw drift tubes [39] placed downstream of the magnet. The tracking system provides a measurement of the momentum,  $p$ , of charged particles with a relative uncertainty that varies from 0.5% at low momentum to 1.0% at 200 GeV/ $c$ . The minimum distance of a track to a primary  $pp$  collision vertex (PV), the impact parameter (IP), is measured with a resolution of  $(15 + 29/p_T)$   $\mu\text{m}$ , where  $p_T$  is the component of the momentum transverse to the beam, in GeV/ $c$ . Different types of charged hadrons are distinguished using information from two ring-imaging Cherenkov detectors [39]. Photons, electrons and hadrons are identified by a calorimeter system consisting of scintillating-pad and preshower detectors, an electromagnetic and a hadronic calorimeter. Muons are identified by a system composed of alternating layers of iron and multiwire proportional chambers [40]. The online event selection is performed by a trigger [39], which consists of a hardware stage, based on information from the calorimeter and muon systems, followed by a software stage, which applies a full event reconstruction. Triggered data further undergo a centralised, offline processing step to deliver physics-analysis-ready data across the entire LHCb physics programme [41].

Simulation is required to model the effects of the detector acceptance, resolution and the imposed selection requirements. In the simulation,  $pp$  collisions are generated using PYTHIA [42] with a specific LHCb configuration [43]. Decays of unstable particles are described by EVTGEN [44], in which final-state radiation is generated using PHOTOS [45]. The interaction of the generated particles with the detector, and its response, are implemented using the GEANT4 toolkit [46] as described in Ref. [47]. Data driven corrections are applied to simulation to account for the small level of mismodelling of the detector occupancy,  $B^+$  momentum,  $B^+$  vertex quality, and particle identification (PID) performance. The momentum of the reconstructed tracks in simulation is also smeared by a small amount to better match the mass resolution of data.

## 4 Data Selection

At first,  $B^+ \rightarrow K^+ \mu^+ \mu^-$  candidates must pass the hardware stage of the trigger. In this stage, at least one muon is required to be above a  $p_T$  threshold between 1.36 GeV/ $c$  and 1.80 GeV/ $c$ , depending on the run period. In the subsequent software stages, at least one of the final state particles is required to have a  $p_T > 1.7$  GeV/ $c$  unless it is a muon, in which case, the condition is  $p_T > 1$  GeV/ $c$ . The final state particles are also required to have an IP  $> 100$   $\mu\text{m}$  with respect to all PVs to reject particles originating directly from the PV. The final stage of the trigger is based on the topology of the signal decay and requires two or more final state particles to form a vertex that is significantly displaced from any PV.

In the offline stage, a signal candidate is formed by combining a track identified as a kaon with a pair of oppositely charged tracks identified as muons. The three tracks are required to have a large IP with respect to all PVs and form a good quality vertex. For the  $B^+$  candidate, the IP with respect to one of the PVs is required to be small, and the decay vertex is required to be significantly displaced from this PV. The angle

between the reconstructed  $B^+$  momentum and the vector connecting the PV to the reconstructed  $B^+$  decay vertex is required to be small. The reconstructed  $B^+$  candidate is also required to have mass,  $m_{K\mu\mu}$ , in the range  $4700(4600) < m_{K\mu\mu} < 7000 \text{ MeV}/c^2$  for Run 2 (Run 1). To reduce backgrounds arising through the misidentification of final-state particles, PID requirements are placed on variables constructed using information from the RICH, calorimeter, and muon subdetectors for all final-state particles.

A source of background, commonly referred to as combinatorial, arises from random combinations of kaons and muons from the underlying event, which happen to pass the selections. To suppress this type of background, a boosted decision tree (BDT) classifier [48, 49] is used. Separate BDTs are trained for Run 1 and Run 2 data-taking periods. During the training, both BDTs use simulated  $B^+ \rightarrow K^+\mu^+\mu^-$  decays as the signal proxy, and  $B^+ \rightarrow K^+\mu^+\mu^-$  candidates in the data with  $m_{K\mu\mu}$  in the region between 5600 and 5900  $\text{MeV}/c^2$  as the background proxy. To avoid potential biases from resonant dimuon modes in the background proxy, candidates close to the  $J/\psi$  and  $\psi(2S)$  resonances are removed. A k-folding procedure [50] with  $k=8$  folds is adopted to train the BDT that uses kinematic and geometric variables, including the variables used in the offline selection stage described above. The variables offering the highest discrimination power include the kinematic properties of the  $B^+$  candidate and the difference in the vertex-fit  $\chi^2$  of the PV when reconstructed with and without the final state particles. The selection on the BDT criterion is chosen to ensure a signal efficiency of 90% for both Run 1 and Run 2 data-taking periods, with a background misidentification rate of about 6% (10%) for Run 1 (Run 2).

Background candidates from  $B$  meson decays with a similar topology to  $B^+ \rightarrow K^+\mu^+\mu^-$  are also present in the data. These originate from pions misidentified as muons from  $B^+ \rightarrow \pi^+(\bar{D}^0 \rightarrow K^+\pi^-)$  decays or a kaon-muon swap from  $B^+ \rightarrow K^+(J/\psi \rightarrow \mu^+\mu^-)$  decays. To reduce these to a negligible level, tighter PID criteria in the specific resonant mass windows are employed. The PID requirements on the muons also reduce background contributions from  $B^+ \rightarrow K^+\pi^+\pi^-$  decays to a negligible level.

## 5 Experimental description of the decay rate

To accurately describe the data, the theoretical  $B^+ \rightarrow K^+\mu^+\mu^-$  decay rate is extended to account for detector response and background contributions. This section describes the efficiency model for the event reconstruction and selection, the detector resolution of the dimuon invariant mass, and the modelling of background contributions.

### 5.1 Efficiency model

The reconstruction and selection requirements placed on the signal candidates result in an efficiency variation across the decay phase space completely described through two variables:  $q^2 \equiv m_{\mu\mu}^2$  and  $\cos\theta_\ell$ , where  $\theta_\ell$  is the angle between the direction of the  $\mu^-$  ( $\mu^+$ ) and the direction of the  $B^+$  ( $B^-$ ) meson in the rest frame of the dimuon system. The most significant efficiency-sculpting effects come from the geometrical acceptance of the detector, the IP requirements on the kaon and muon tracks, and the  $p_T$  requirement of the trigger. The efficiency function,  $\mathcal{E}(q^2, \cos\theta_\ell)$ , is determined using simulated  $B^+ \rightarrow K^+\mu^+\mu^-$  decays passing the entire selection chain and corrected for differences between data and simulation

that are associated with the modelling of the trigger efficiency, PID performance, and  $B^+$  meson kinematic distributions, using control samples in the data. Each of these simulated candidates is assigned a weight according to the phase-space density in  $q^2$  and  $\cos\theta_\ell$ .

This analysis is performed by integrating over  $\cos\theta_\ell$  such that the fully selected  $B^+ \rightarrow K^+\mu^+\mu^-$  candidates are described by the efficiency-corrected decay rate given by

$$\left. \frac{d^2\Gamma_\mu}{dq^2} \right|_{\text{eff}} \equiv \int \frac{d^2\Gamma_\mu}{dq^2 d\cos\theta_\ell} \mathcal{E}(q^2, \cos\theta_\ell) d\cos\theta_\ell. \quad (18)$$

with

$$\begin{aligned} \frac{d^2\Gamma_\mu}{dq^2 d\cos\theta_\ell} \propto & |\mathbf{k}|\beta_+ \left\{ |\mathbf{k}|^2\beta_+^2(1 - \cos^2\theta_\ell)|C_A|^2 f_+^2(q^2) \right. \\ & + \frac{m_\mu^2(M_B^2 - M_K^2)^2}{q^2 M_B^2} |C_A|^2 f_0^2(q^2) \\ & \left. + |\mathbf{k}|^2(1 - \beta_+^2 \cos^2\theta_\ell) \left| C_V^{\text{eff}} + 2(C_7^{\text{eff}} + C_7') \frac{m_b + m_s}{M_B + M_K} \frac{f_T(q^2)}{f_+(q^2)} \right|^2 f_+^2(q^2) \right\}, \end{aligned} \quad (19)$$

where  $C_V^{\text{eff}} \equiv C_9^{\text{eff}} + C_9'$  and, following Ref. [4], we assume no scalar, pseudoscalar, or tensor Wilson coefficients that give rise to an angular term proportional to  $\cos\theta_\ell$  [51]. Therefore, from Eqs. 18 and 19, the integral of the efficiency-corrected decay rate over  $\cos\theta_\ell$  is broken up into three terms with different  $\cos\theta_\ell$ , Wilson coefficient and form-factor dependence. These terms are given by

$$\mathcal{E}_{+C_A}(q^2) = \frac{\int_{-1}^{+1} \mathcal{E}(q^2, \cos\theta_\ell)(1 - \cos^2\theta_\ell) d\cos\theta_\ell}{\int_{-1}^{+1} (1 - \cos^2\theta_\ell) d\cos\theta_\ell}, \quad (20)$$

$$\mathcal{E}_{0C_A}(q^2) = \frac{\int_{-1}^{+1} \mathcal{E}(q^2, \cos\theta_\ell) d\cos\theta_\ell}{\int_{-1}^{+1} d\cos\theta_\ell}, \quad (21)$$

$$\mathcal{E}_{+C_V}(q^2) = \frac{\int_{-1}^{+1} \mathcal{E}(q^2, \cos\theta_\ell)(1 - \beta_+^2 \cos^2\theta_\ell) d\cos\theta_\ell}{\int_{-1}^{+1} (1 - \beta_+^2 \cos^2\theta_\ell) d\cos\theta_\ell}. \quad (22)$$

The denominator of these efficiency functions is defined such that the efficiency-corrected differential decay rate,  $\left. \frac{d^2\Gamma_\mu}{dq^2} \right|_{\text{eff}}$ , is obtained by multiplying each of the three terms on the right-hand side of Eq. 2 by the corresponding efficiency function given in Eqs. 20, 21, 22. The efficiencies are determined separately for Run 1 and Run 2 data-taking periods and averaged according to the ratio of yields of fully selected  $B^+ \rightarrow K^+(J/\psi \rightarrow \mu^+\mu^-)$  in each period. The efficiency distributions defined in Eqs. 20, 21, 22 are shown in Fig. 1. Each of these three efficiency distributions is parametrised using a fourth-order polynomial in  $m_{\mu\mu}$ .

## 5.2 Resolution model

To improve the dimuon-mass resolution, a kinematic fit is performed for each selected  $B^+$  candidate constraining the reconstructed  $m_{K\mu\mu}$  to the known  $B^+$  mass [30] and requiring

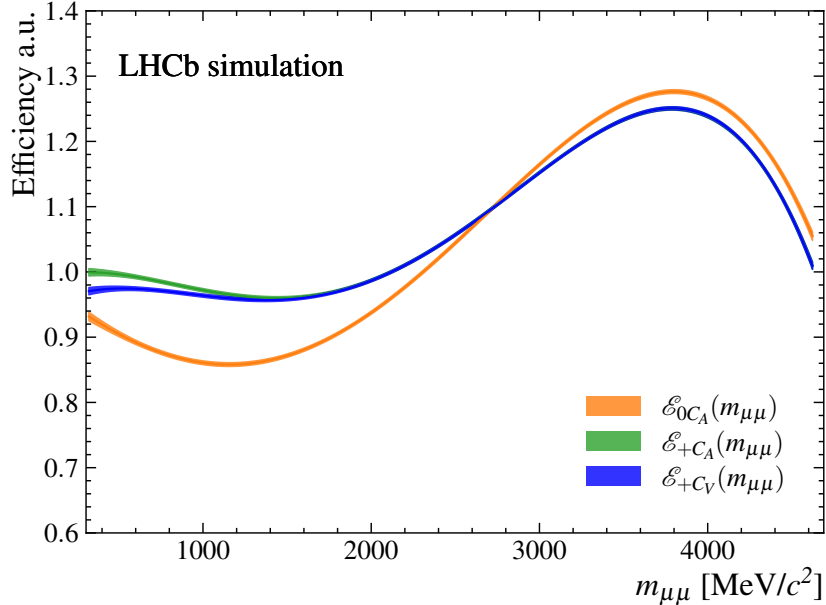


Figure 1: The efficiency functions  $\mathcal{E}_{+C_A}$ ,  $\mathcal{E}_{0C_A}$ , and  $\mathcal{E}_{+C_V}$  given in Eqs. 20, 21, and 22 respectively. The bands represent the statistical uncertainty due to the size of the simulation sample.

Table 2: The three regions chosen for the convolution and the dominant resonance within the region.

	$m_{\mu\mu}^{\text{rec}}$ range [MeV/ $c^2$ ]	Dominant resonance
Region-1	300 to 1800	$\phi(1020)$
Region-2	1800 to 3400	$J/\psi$
Region-3	3400 to 4700	$\psi(2S)$

the  $B^+$  candidate to originate from one of the PVs in the event. The kinematically constrained dimuon mass is denoted as  $m_{\mu\mu}^{\text{rec}}$ . After this constraint, the detector resolution varies between 2 and 7 MeV/ $c^2$ , depending on dimuon mass, and needs to be taken into account when determining parameters of interest. To account for this, the  $B^+ \rightarrow K^+ \mu^+ \mu^-$  phase space is split into three  $m_{\mu\mu}^{\text{rec}}$  regions each containing a dominant resonance as shown in Table 2. A sum of a Gaussian function with power-law tails on either side of the peak [52] and a second Gaussian function with the same peak position is used as the resolution model. This model is validated on simulation for  $J/\psi$  and  $\psi(2S)$  mesons but all the resolution parameters are extracted from data, except for region-1. In this region migration effects from narrow resonances, such as the  $\phi(1020)$ , are far smaller compared to those in regions-2 and -3, and the resolution parameters are therefore obtained from simulation.

The efficiency-corrected decay rate is convolved with the resolution models to give the experimental description of the signal decay rate as a function of the reconstructed dimuon mass,

$$P^{\text{sig}}(m_{\mu\mu}^{\text{rec}}) = \mathcal{R}(m_{\mu\mu}^{\text{rec}}, m_{\mu\mu}) \otimes \left[ 2m_{\mu\mu} \left. \frac{d\Gamma_{\mu}}{dq^2} \right|_{\text{eff}} \right]. \quad (23)$$

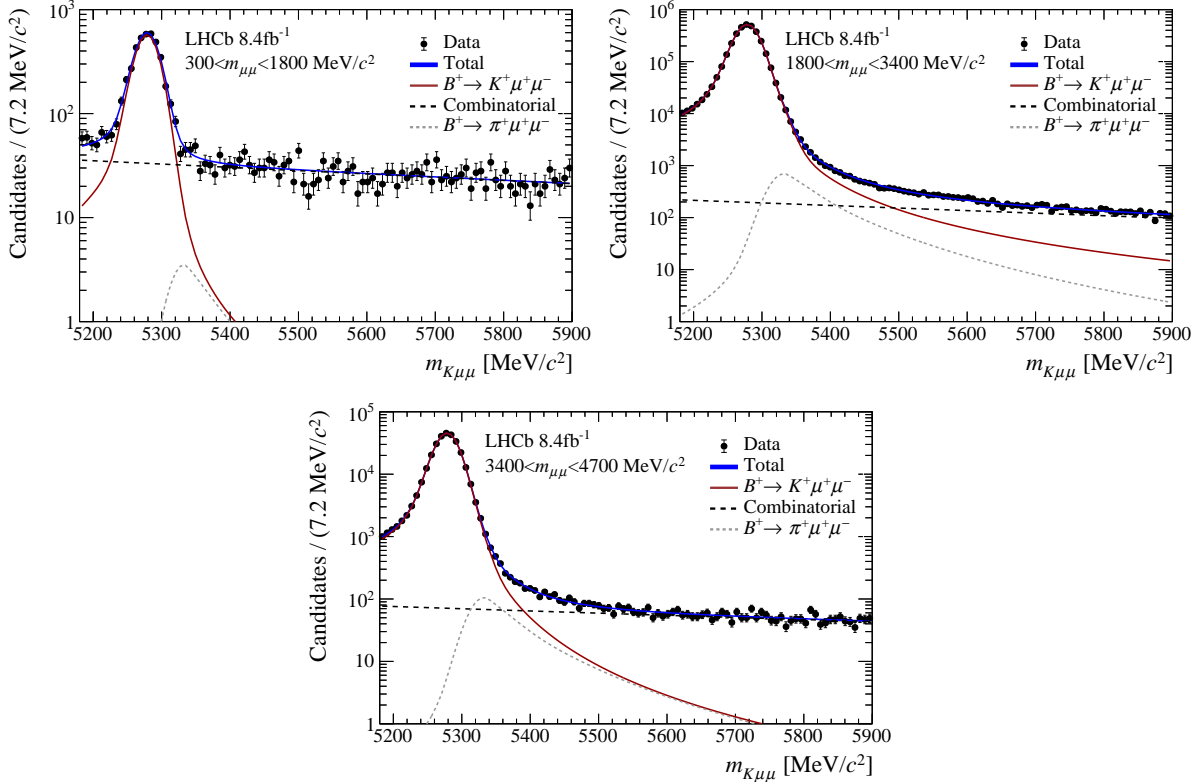


Figure 2: The fit to the reconstructed  $m_{K\mu\mu}$  mass distribution in (top left) region-1, (top right) region-2, and (bottom) region-3 corresponding to the  $m_{\mu\mu}$  ranges defined in Table 2.

Here  $\mathcal{R}(m_{\mu\mu}^{\text{rec}}, m_{\mu\mu})$  is one of the three resolution models depending on the region  $m_{\mu\mu}^{\text{rec}}$ . The factor  $2m_{\mu\mu}$  is the conversion factor from  $dq^2$  to  $dm_{\mu\mu}$  and  $\left. \frac{d\Gamma_{\mu}}{dq^2} \right|_{\text{eff}}$  is the efficiency corrected differential decay rate from Eq. 18.

### 5.3 Modelling the background contributions

The residual backgrounds surviving the selection criteria are the combinatorial background and the backgrounds involving pions misidentified as kaons from  $B^+ \rightarrow \pi^+ \mu^+ \mu^-$  decays. The yields of these backgrounds are estimated from unbinned maximum-likelihood fits to the reconstructed  $m_{K\mu\mu}$  mass. The model of the  $m_{K\mu\mu}$  distribution depends on the dimuon mass distribution. Therefore, the signal and background yields are extracted in the three regions of dimuon mass shown in Table 2.

The reconstructed  $m_{K\mu\mu}$  distribution for the three dimuon mass regions are shown in Fig. 2. An exponential function is used to model the combinatorial background and a Gaussian distribution with power law tails [52] is used to model the misidentified pion background, whose shape parameters are extracted from simulated  $B^+ \rightarrow \pi^+ \mu^+ \mu^-$  candidates. The signal shape in  $m_{K\mu\mu}$  is modelled using a Gaussian function with power-law tails added and two other Gaussian functions all with shared peak positions. The peak position and width parameters are determined from the fit to the data while the tail parameters are fixed to values determined from simulation.

The fit to the  $m_{\mu\mu}^{\text{rec}}$  distribution is performed for candidates with  $m_{K\mu\mu}$  within a signal

window of  $\pm 40 \text{ MeV}/c^2$  of the known  $B^+$  mass. The fits to the  $m_{K\mu\mu}$  distribution in the data are used to determine the signal and background fractions within this window. Kernel density estimators (KDEs) [53] are used to model the  $m_{\mu\mu}$  shapes of misidentified  $B^+ \rightarrow \pi^+(J/\psi \rightarrow \mu^+\mu^-)$  and  $B^+ \rightarrow \pi^+(\psi(2S) \rightarrow \mu^+\mu^-)$  decays in the simulation. The contribution of misidentified pions from the decay of  $B^+ \rightarrow \pi^+\mu^+\mu^-$  within the  $m_{K\mu\mu}$  signal window is negligible and is therefore ignored.

Combinatorial  $B^+ \rightarrow K^+\mu^+\mu^-$  candidates comprise three components: a combinatorial  $K^+$  with a genuine  $J/\psi$  candidate (combinatorial  $J/\psi$ ); a combinatorial  $K^+$  with a genuine  $\psi(2S)$  candidate (combinatorial  $\psi(2S)$ ); and a three-particle fully-combinatorial  $K^+\mu^+\mu^-$  component (fully combinatorial). The shape of each combinatorial background contribution in  $m_{\mu\mu}^{\text{rec}}$  is obtained from the  $m_{K\mu\mu}$  upper-mass sideband defined as  $5440(5460) < m_{K\mu\mu} < 5840(5860) \text{ MeV}/c^2$  for the Run 2 (Run 1) data-taking periods. These regions are dominated by combinatorial background candidates with small contributions from  $B^+ \rightarrow K^+\mu^+\mu^-$  and  $B^+ \rightarrow \pi^+\mu^+\mu^-$  decays. The kinematic constraint introduces a dependence between the  $m_{K\mu\mu}$  distribution and the kinematically constrained  $m_{\mu\mu}^{\text{rec}}$  distribution. Therefore, in order to model this dependence, the upper-mass sideband is split into five  $80 \text{ MeV}/c^2$ -wide  $m_{K\mu\mu}$  regions with the kinematic constraint applied to the centre of each region, and the dimuon mass is recomputed using this kinematic constraint. The kinematically constrained  $m_{\mu\mu}^{\text{rec}}$  data in each of these five regions is fitted using unbinned maximum-likelihood estimators. An ARGUS function [54] is used to model the continuum combinatorial background, the sum of two Gaussian functions for the  $J/\psi$  combinatorial background, and a single Gaussian function for  $\psi(2S)$  combinatorial background. The combinatorial background parameters describing the  $m_{\mu\mu}^{\text{rec}}$  shape include the ARGUS shape parameter, the masses and widths of the Gaussians describing the  $J/\psi$  and  $\psi(2S)$  contributions, and the fraction between the two Gaussians used to model the  $J/\psi$  combinatorial component. The  $m_{\mu\mu}^{\text{rec}}$  distribution of  $B^+ \rightarrow K^+\mu^+\mu^-$  and  $B^+ \rightarrow \pi^+\mu^+\mu^-$  decays misreconstructed in the upper-mass sideband are modelled using KDEs determined from simulation in each of the  $m_{K\mu\mu}$  upper-mass sideband regions. The yields of these misreconstructed components are constrained to their expected values from the fit to the  $m_{K\mu\mu}$  distribution in the data. These parameters and the fraction of combinatorial  $J/\psi$  and  $\psi(2S)$  over the total combinatorial background are extrapolated linearly to the known  $B^+$  mass giving the shape of the combinatorial background. The shapes of the background from the two run periods are added together weighted by the background yields in the signal region. The total model is given by the sum of the signal and background components, where the signal fraction is obtained from the fits to the  $m_{K\mu\mu}$  distribution in each of the three  $m_{\mu\mu}^{\text{rec}}$  regions.

## 6 Systematic uncertainties

The lattice QCD precision in the local  $B \rightarrow K$  form factors is an important source of systematic uncertainty. These form-factor uncertainties are propagated into the likelihood through an external multivariate Gaussian constraint on the form-factor coefficients, provided by the different lattice QCD calculations [36, 37]. Similarly, the uncertainties on the masses and widths of the broad resonances above the open-charm threshold are propagated into the likelihood through Gaussian constraints provided in Ref. [55].

Another important source of systematic uncertainty originates from the precision of

the measured branching fraction of  $B^+ \rightarrow K^+ J/\psi$  decays as taken from Ref. [56]. The size of this contribution is evaluated by repeating the fit with the branching fraction of the  $B^+ \rightarrow K^+ J/\psi (\rightarrow \mu^+ \mu^-)$  decay varied according to its uncertainty. The RMS of the resulting distribution of each parameter of interest, along with the linear correlations of these variations between the parameters, comprise the covariance matrix of the systematic uncertainty.

The effect of using three distinct resolution functions in the fit instead of a single resolution function with a continuous dependence on the dimuon mass is estimated using pseudoexperiments. Each pseudoexperiment is generated using a model based on the best fit point in the data, without any convolution applied, and then smeared using two different sets of resolution models: one that accounts for the continuous dependence of the resolution on dimuon mass, and another following the baseline procedure of three separate resolution functions in each of the three dimuon mass regions. Both sets of pseudodata are then fitted with the baseline fit model. The systematic covariance matrix of the parameters of interest is evaluated by taking the RMS width of the distribution resulting from the differences between the two fit results for each parameter of interest, along with the linear correlations in between the parameter variations.

The statistical precision of the background model is propagated to the parameters of interest by bootstrapping the upper-mass sideband data, varying the signal fractions according to their covariances in each dimuon mass region, and repeating the background fit procedure outlined in Sec. 5.3. The RMS and bias of the fitted parameter distribution are combined in quadrature, and the linear correlations among parameter variations are used to construct the covariance matrix of this systematic uncertainty.

The uncertainty on the subtraction constant  $Y_{cc}^0 = 0.230 \pm 0.065$  [13] is propagated directly to  $C_9$  and is entirely uncorrelated with other parameters of interest. Other systematic uncertainties that were studied and found to be negligible include the statistical precision of the efficiency model, the choice of the efficiency parametrisation, and the impact of the corrections applied to the simulation.

Table 3 summarises the size of the sources of systematic uncertainty described in this section. The systematic uncertainty from the precision of the  $B \rightarrow K$  form factors determined by the HPQCD collaboration [36] is indicative and directly encoded in the likelihood surface. The total systematic uncertainty is obtained by adding up the systematic covariance matrices and smearing the one- and two-dimensional likelihood profiles presented in Sec. 7.

## 7 Results and discussion

An unbinned log-likelihood fit is performed to the dimuon spectrum of  $B^+ \rightarrow K^+ \mu^+ \mu^-$  candidates using the signal and background models described in Sec. 5. The parameters of interest of the fit are the Wilson coefficients  $C_V$ ,  $C_A$ , and the magnitudes and phases of the nonlocal amplitudes. The baseline fit relies on the most recent and precise lattice QCD determinations of the  $B^+ \rightarrow K^+$  local form factors provided by the HPQCD collaboration [36], while an alternative fit using local  $B \rightarrow K$  form factors by the FNAL/MILC collaboration [37] is also explored.

Similarly to what was reported in the previous iteration of this analysis [3], the negative log-likelihood exhibits four near-degenerate minima depending on the signs of the  $J/\psi$

Table 3: Systematic uncertainties on the parameters of interest. See text for further information. The systematic uncertainty associated with the precision of the HPQCD  $B \rightarrow K$  form factors are indicative, as this uncertainty is directly encoded in the likelihood.

Parameter	HPQCD FF	$\mathcal{B}(B^+ \rightarrow J/\psi K^+)$	Resolution	Bkg extrapolation	Subtraction
$C_V$	0.141	0.079	0.013	0.012	0.065
$C_A$	0.084	0.014	0.034	0.031	–
$\delta_{\rho(770)}$ [rad]	0.074	0.002	0.016	0.005	–
$\eta_{\rho(770)}$	0.012	0.001	0.001	0.001	–
$\delta_{\omega(782)}$ [rad]	0.006	0.015	0.018	0.001	–
$\eta_{\omega(782)}$	0.058	0.005	0.009	0.001	–
$\delta_{\phi(1020)}$ [rad]	0.005	0.051	0.004	0.002	–
$\eta_{\phi(1020)}$	0.082	0.004	0.010	0.001	–
$\delta_{J/\psi}$ [rad]	0.018	0.001	0.002	0.006	–
$\delta_{\psi(2S)}$ [rad]	0.027	0.006	0.006	0.012	–
$\eta_{\psi(2S)}$	41.42	18.69	0.020	0.087	–
$\delta_{\psi(3770)}$ [rad]	0.030	0.002	0.003	0.011	–
$\eta_{\psi(3770)}$	0.099	0.035	0.006	0.040	–
$\delta_{\psi(4040)}$ [rad]	0.098	0.003	0.006	0.018	–
$\eta_{\psi(4040)}$	0.135	0.015	0.009	0.006	–
$\delta_{\psi(4160)}$ [rad]	0.107	0.002	0.007	0.009	–
$\eta_{\psi(4160)}$	0.118	0.023	0.013	0.010	–
$\delta_{\psi(4415)}$ [rad]	0.085	0.002	0.016	0.010	–
$\eta_{\psi(4415)}$	0.072	0.016	0.027	0.009	–
$\delta_{2p}$ [rad]	0.207	0.003	0.035	0.017	–
$\eta_{2p}$	0.137	0.002	0.005	0.021	–

and  $\psi(2S)$  resonance phases. The  $m_{\mu\mu}^{\text{rec}}$  distribution of  $B^+ \rightarrow K^+ \mu^+ \mu^-$  decays, along with the best-fit model to the data for all four near-degenerate minima, is shown in Fig. 3.

The solution with the lowest negative log-likelihood is found for a negative  $J/\psi$  phase and a positive  $\psi(2S)$  phase relative to the local amplitude, with a small destructive quantum-mechanical interference in the decay rate. Table 4 presents the changes in the negative log-likelihood and Wilson coefficients  $C_V$  and  $C_A$  in all four quadrants relative to the quadrant with the lowest negative log-likelihood. The Wilson coefficients remain essentially identical for all four solutions. In contrast, the nonlocal parameters, presented in Table 5, vary between the solutions. Similarly to the measurement of the nonlocal amplitudes in  $B^0 \rightarrow K^{*0} \mu^+ \mu^-$  decays presented in Ref. [28], there is no evidence of two-particle nonlocal contributions from  $B^+ \rightarrow (D^{(*)} \bar{D}^{(*)} \rightarrow \mu^+ \mu^-) K^+$  transitions in the spectrum of  $B^+ \rightarrow K^+ \mu^+ \mu^-$  decays.

As discussed in Sec. 2, the number of  $B^+ \rightarrow K^+ \mu^+ \mu^-$  candidates available in the Run 1 and Run 2 datasets of the LHCb experiment does not allow for the determination of all three two-particle amplitudes. Instead, an effective amplitude is used, in which all three  $D\bar{D}$ ,  $D\bar{D}^*$ , and  $D^*\bar{D}^*$  components share the same magnitude and phase. Although this choice has a negligible impact on the couplings  $C_V$  and  $C_A$ , it hinders an accurate

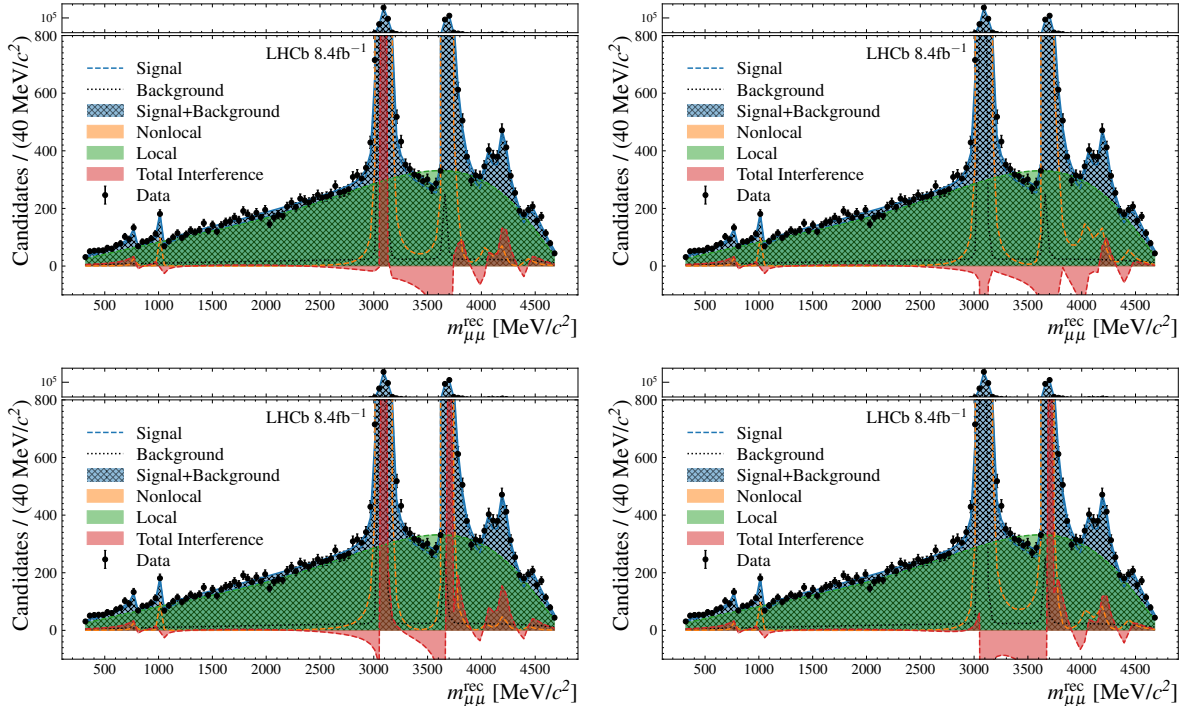


Figure 3: Fit to the  $m_{\mu\mu}^{\text{rec}}$  distribution using form factors from the HPQCD collaboration [36] for: (top left) negative  $J/\psi$  phase, positive  $\psi(2S)$  phase; (top right) positive  $J/\psi$  phase, positive  $\psi(2S)$  phase; (bottom left) negative  $J/\psi$  phase, negative  $\psi(2S)$  phase; (bottom right) positive  $J/\psi$  phase, negative  $\psi(2S)$  phase.

Table 4: Changes to the negative log-likelihood and Wilson coefficients relative to the deepest minimum for all four-fold degenerate solutions in  $\delta_{J/\psi}$  and  $\delta_{\psi(2S)}$  phases. The four fit results are denoted as  $(-, +)$ ,  $(+, +)$ ,  $(-, -)$ ,  $(+, -)$ , where the first (second) sign in each pair represents the sign of  $\delta_{J/\psi}$  ( $\delta_{\psi(2S)}$ ) phase. The values of  $C_V$  and  $C_A$  are calculated relative to the result in the lowest negative log-likelihood phase quadrant  $(-, +)$ .

Parameter	$(-, +)$	$(+, +)$	$(-, -)$	$(+, -)$
$-2\Delta \log \mathcal{L}^{\text{min}}$	0	0.09	0.69	0.463
$ \Delta C_V $	0	0.006	0.006	0.014
$ \Delta C_A $	0	0.001	0.011	0.012

determination of  $C_9^\tau$  entering through the two-particle nonlocal amplitude of the process  $B^+ \rightarrow (\tau^+\tau^- \rightarrow \mu^+\mu^-)K^+$ .

## 7.1 Measurement of Wilson coefficients

The two-dimensional likelihood surface for  $C_V$  and  $C_A$ , including all systematic uncertainties, is shown in Fig. 4. The branching fraction of the short-distance component provides a strong constraint on the combination  $C_V^2 + C_A^2$ , as shown in Eq. 2, resulting in the annular structure of the likelihood profile in Fig. 4. The fit distinguishes between  $C_V$  and  $C_A$  through the interference of  $C_V$  with the nonlocal amplitudes. For comparison, the

Table 5: Measured values of the nonlocal parameters in the different  $(\delta_{J/\psi}, \delta_{\psi(2S)})$  quadrants. The four fit results are denoted as  $(-, +)$ ,  $(+, +)$ ,  $(-, -)$ ,  $(+, -)$  where the first (second) sign in each pair represents the sign of  $\delta_{J/\psi}$  ( $\delta_{\psi(2S)}$ ) phase. The first uncertainty is statistical while the second is systematic.

Parameter	$(-, +)$	$(+, +)$	$(-, -)$	$(+, -)$
$\delta_{\rho(770)}$ [rad]	$-0.48 \pm 0.36 \pm 0.02$	$-0.47 \pm 0.36 \pm 0.02$	$-0.49 \pm 0.36 \pm 0.02$	$-0.48 \pm 0.36 \pm 0.02$
$\eta_{\rho(770)}$	$0.69 \pm 0.06 \pm 0.00$	$0.69 \pm 0.07 \pm 0.00$	$0.69 \pm 0.06 \pm 0.00$	$0.69 \pm 0.06 \pm 0.00$
$\delta_{\omega(782)}$ [rad]	$-0.08 \pm 0.26 \pm 0.02$	$-0.07 \pm 0.26 \pm 0.02$	$-0.08 \pm 0.26 \pm 0.02$	$-0.07 \pm 0.26 \pm 0.02$
$\eta_{\omega(782)}$	$4.65 \pm 0.29 \pm 0.01$	$4.64 \pm 0.36 \pm 0.01$	$4.65 \pm 0.31 \pm 0.01$	$4.65 \pm 0.32 \pm 0.01$
$\delta_{\phi(1020)}$ [rad]	$0.38 \pm 0.31 \pm 0.05$	$0.40 \pm 0.31 \pm 0.05$	$0.38 \pm 0.30 \pm 0.05$	$0.40 \pm 0.30 \pm 0.05$
$\eta_{\phi(1020)}$	$12.77 \pm 0.87 \pm 0.01$	$12.77 \pm 0.96 \pm 0.01$	$12.77 \pm 0.87 \pm 0.01$	$12.77 \pm 0.91 \pm 0.01$
$\delta_{J/\psi}$ [rad]	$-1.56 \pm 0.06 \pm 0.01$	$1.60 \pm 0.05 \pm 0.01$	$-1.70 \pm 0.07 \pm 0.01$	$1.45 \pm 0.04 \pm 0.01$
$\delta_{\psi(2S)}$ [rad]	$2.21 \pm 0.16 \pm 0.01$	$1.77 \pm 0.13 \pm 0.01$	$-2.02 \pm 0.13 \pm 0.01$	$-2.46 \pm 0.11 \pm 0.01$
$\eta_{\psi(2S)}$ ( $\times 10^3$ )	$1.23 \pm 0.03 \pm 0.02$	$1.23 \pm 0.03 \pm 0.02$	$1.23 \pm 0.03 \pm 0.03$	$1.24 \pm 0.04 \pm 0.02$
$\delta_{\psi(3770)}$ [rad]	$2.90 \pm 0.17 \pm 0.01$	$2.50 \pm 0.35 \pm 0.01$	$-2.56 \pm 0.18 \pm 0.01$	$-2.96 \pm 0.13 \pm 0.01$
$\eta_{\psi(3770)}$	$2.92 \pm 0.43 \pm 0.05$	$2.93 \pm 0.68 \pm 0.05$	$2.68 \pm 0.40 \pm 0.05$	$2.72 \pm 0.31 \pm 0.05$
$\delta_{\psi(4040)}$ [rad]	$-3.11 \pm 0.19 \pm 0.02$	$2.86 \pm 0.32 \pm 0.02$	$-2.82 \pm 0.18 \pm 0.02$	$-3.14 \pm 0.17 \pm 0.02$
$\eta_{\psi(4040)}$	$1.50 \pm 0.26 \pm 0.02$	$1.52 \pm 0.30 \pm 0.02$	$1.45 \pm 0.25 \pm 0.02$	$1.46 \pm 0.25 \pm 0.02$
$\delta_{\psi(4160)}$ [rad]	$-2.31 \pm 0.18 \pm 0.01$	$-2.60 \pm 0.32 \pm 0.01$	$-2.08 \pm 0.17 \pm 0.01$	$-2.37 \pm 0.18 \pm 0.01$
$\eta_{\psi(4160)}$	$2.04 \pm 0.26 \pm 0.03$	$2.05 \pm 0.32 \pm 0.03$	$2.02 \pm 0.25 \pm 0.03$	$2.03 \pm 0.24 \pm 0.03$
$\delta_{\psi(4415)}$ [rad]	$2.56 \pm 0.32 \pm 0.02$	$2.32 \pm 0.47 \pm 0.02$	$2.70 \pm 0.30 \pm 0.02$	$2.45 \pm 0.25 \pm 0.02$
$\eta_{\psi(4415)}$	$1.62 \pm 0.32 \pm 0.03$	$1.64 \pm 0.37 \pm 0.03$	$1.59 \pm 0.33 \pm 0.03$	$1.61 \pm 0.34 \pm 0.03$
$\delta_{2p}$ [rad]	$-2.41 \pm 0.56 \pm 0.04$	$-2.63 \pm 0.79 \pm 0.04$	$-2.29 \pm 0.60 \pm 0.04$	$-2.49 \pm 0.47 \pm 0.04$
$\eta_{2p}$	$0.30 \pm 0.16 \pm 0.02$	$0.28 \pm 0.20 \pm 0.02$	$0.32 \pm 0.20 \pm 0.02$	$0.31 \pm 0.14 \pm 0.02$

corresponding determination obtained using the FNAL/MILC  $B \rightarrow K$  local form factors from Ref. [37] is also displayed. When employing the HPQCD local form factors for  $B \rightarrow K$  transitions, the extracted Wilson coefficients exhibit a tension with the Standard Model at the level of  $4.0\sigma$ . The results obtained using the FNAL/MILC form factors are fully consistent with those derived from the HPQCD calculation, although as expected, the larger uncertainties associated with the FNAL/MILC form factors reduce the significance of the deviation from the Standard Model prediction to  $1.6\sigma$ .

For both HPQCD and FNAL/MILC form factors, the fit to the data prefers values for  $C_{V,A}$  larger than  $C_{V,A}^{\text{SM}}$ . Assuming SM values for  $C'_9 = C'_{10} = 0$  and  $C_{10} = -4.166$ , the data prefer  $C_9 < C_9^{\text{SM}}$ , as shown by the likelihood profiles of Fig. 5. The one-dimensional profile of  $C_9$  obtained using HPQCD local form factors yields a value consistent with global analyses of  $b \rightarrow s\mu^+\mu^-$  transitions that indicate potential new physics contributions to  $C_9$  (e.g. Ref. [25]). The observed shift, however, is smaller than that reported in Ref. [13], based solely on  $B^+ \rightarrow K^+\mu^+\mu^-$  differential branching fraction measurements from Run 1 of the LHCb experiment and Run 2 of the CMS experiment.

## 7.2 The differential branching fraction

The differential branching fraction is constructed out of the local and nonlocal amplitudes and compared to the direct measurement from the LHCb collaboration using  $3 \text{ fb}^{-1}$  of Run 1

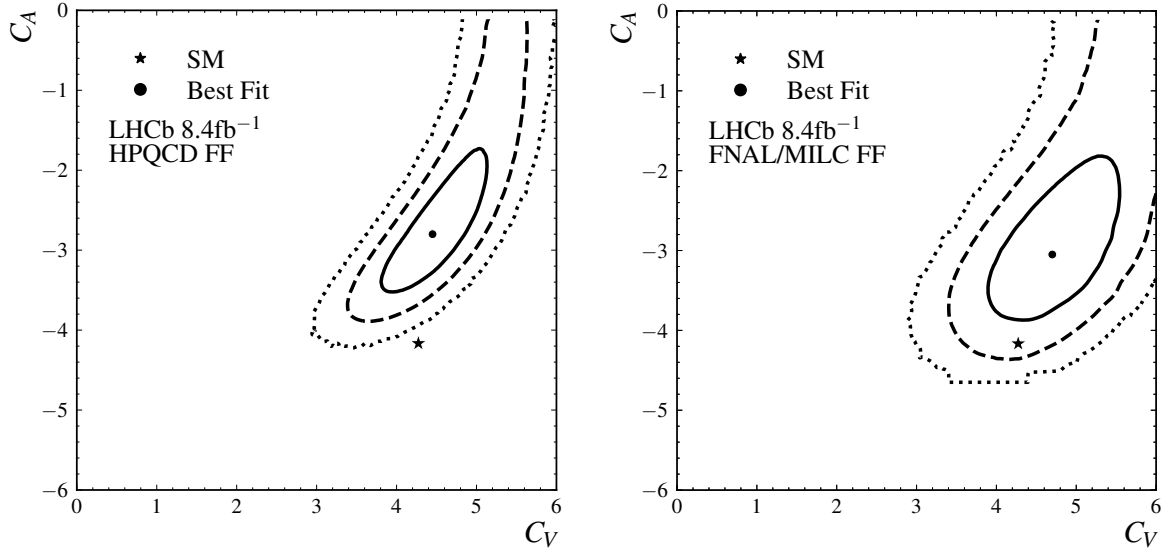


Figure 4: Likelihood profiles of  $C_V$  and  $C_A$  resulting from a fit to the data using the  $B^+ \rightarrow K^+$  local form-factor determination from (left) the HPQCD collaboration [36] and (right) the FNAL/MILC collaboration [37]. The different curves correspond to the 68.3%, 95.4% and 99.7% confidence intervals that include systematic uncertainties. The SM point is shown as a star.

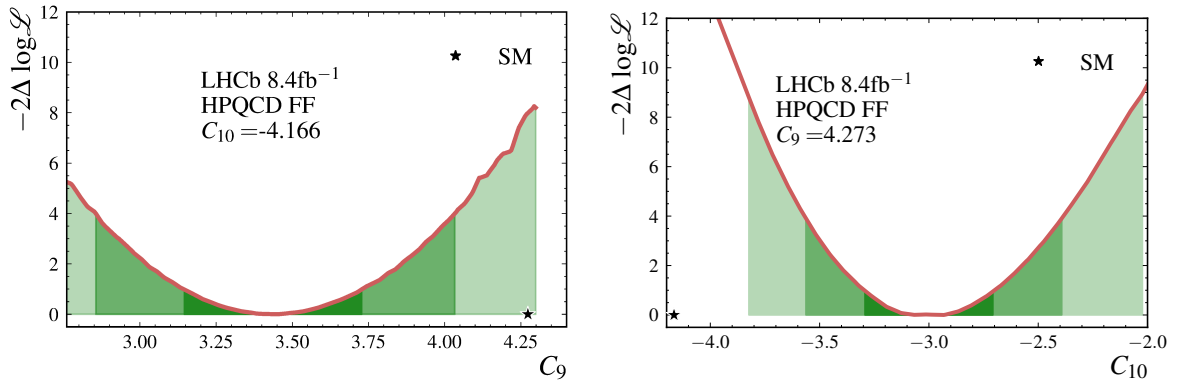


Figure 5: Likelihood profile of (left)  $C_9$  while fixing  $C_{10}$  to the SM value, and (right)  $C_{10}$  while fixing  $C_9$  to the SM value. In both cases,  $C'_9$  and  $C'_{10}$  are set to their SM value of zero, and the HPQCD local form-factor computations are used. The 68.3%, 95.4% and 99.7% confidence intervals are indicated as green bands and include systematic uncertainties. The SM point (star) is also shown.

data [8] as shown in Fig. 6. A good agreement is seen between the two determinations. Figure 6 also shows the effect of the nonlocal amplitude and its interference with the local part in the  $B^+ \rightarrow K^+ \mu^+ \mu^-$  decay rate. In the region  $1.5 < q^2 < 8.0 \text{ GeV}^2/c^4$  the nonlocal effects are minor, but become important outside this region.

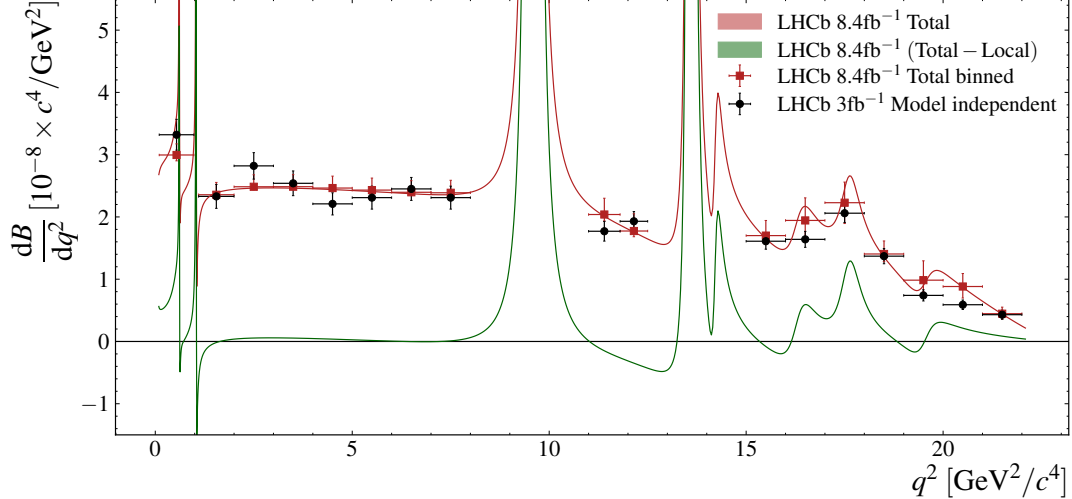


Figure 6: Measured differential branching fraction of the  $B^+ \rightarrow K^+ \mu^+ \mu^-$  decay shown using the model described in this paper in an unbinned manner (maroon solid curve) and evaluated in  $q^2$  bins (maroon squares with error bars). The contribution of the nonlocal amplitude (green), obtained by subtracting the decay rate associated with the local contribution from the total decay rate, is also displayed. The shaded bands represent the 68.3% confidence intervals derived from variations of the fit parameters according to the full covariance matrix, incorporating both statistical and systematic uncertainties. For comparison, the model-independent  $q^2$ -binned measurement reported by the LHCb collaboration in Ref. [8] (black circles) is also shown.

### 7.3 Introducing a $q^2$ -dependent term to Wilson coefficients $C_V$ and $C_A$

To check for any residual  $q^2$ -dependent nonlocal contribution to  $C_V$  and  $C_A$ , alternative fits with  $q^2$ -dependent Wilson coefficients are performed. For these fits the Wilson coefficients are reparametrised with a linear dependence on  $q^2$  as

$$C_V^{q^2} = C_V + a(q^2 - 11.09 \text{ GeV}^2/c^4), \quad C_A^{q^2} = C_A + b(q^2 - 11.09 \text{ GeV}^2/c^4), \quad (24)$$

with  $a$  and  $b$  being the newly introduced fit parameters. The point  $11.09 \text{ GeV}^2/c^4$  is chosen as it is the midpoint of the considered  $q^2$  phase space. This fit is performed in two variations, where either  $a$  or  $b$  is treated as a fit parameter. In addition, a step-like dependence on  $C_V$  is also investigated and given by the ansatz,

$$C_V^{\text{step}} = C_V + \Delta \left( \frac{e^x}{1 + e^x} - \frac{1}{2} \right) \text{ with } x = \frac{m_{\mu\mu} - m_t}{100 \text{ MeV}/c^2} \quad (25)$$

where  $\Delta$  is the newly introduced fit parameter and  $m_t = 3096.65 \text{ MeV}/c^2$  ( $J/\psi$  peak), or  $m_t = 3871.70 \text{ MeV}/c$  ( $D\bar{D}^*$  threshold). The results of the fits introducing a linear  $q^2$  dependence to  $C_V$  or  $C_A$  are  $a = 0.078 \pm 0.052 (\text{GeV}^2/c^4)^{-1}$  and  $b = -0.090 \pm 0.045 (\text{GeV}^2/c^4)^{-1}$ . The introduction of a step-like behaviour in  $C_V$  with a threshold at  $3096.65 \text{ MeV}/c^2$  results in  $\Delta_{J/\psi} = 0.41 \pm 0.24$ , and with a threshold at  $3871.70 \text{ MeV}/c^2$  in  $\Delta_{D\bar{D}^*} = -1.37 \pm 0.53$ .

Given the precision of the  $q^2$ -dependent parameters, there is a preference for a residual  $q^2$  dependence in  $C_A$  at the level of  $2\sigma$ . The value and significance of this parameter are similar to those obtained by the corresponding amplitude analysis in  $B^0 \rightarrow K^{*0} \mu^+ \mu^-$

decays presented in Ref. [28]. Alternatively, there is an indication of a threshold effect in  $C_V$  above the open-charm threshold at a significance of  $2.6\sigma$ . The systematic uncertainties described in Sec. 6 have a negligible effect on these significances.

## 8 Conclusions

Using data collected with the LHCb detector corresponding to an integrated luminosity of  $8.4\text{fb}^{-1}$ , an analysis of the local and nonlocal contributions to the  $B^+ \rightarrow K^+\mu^+\mu^-$  decay rate has been performed. The nonlocal amplitudes are modelled with a dispersion-relation approach that incorporates both one-particle and two-particle contributions. This represents a significant improvement over the treatment of nonlocal effects in previous LHCb analyses of these decays.

Using the latest lattice QCD computations of the  $B \rightarrow K$  local form factors from the HPQCD collaboration, the values of the couplings  $C_V$  and  $C_A$  are found to be in tension with the SM prediction at the  $4.0\sigma$  level. Under the assumption of no new physics contributions to  $C'_9$  and  $C'_{10}$  and  $C_{10}$ , the measured value of  $C_9$  is compatible with global analyses of  $b \rightarrow s\mu^+\mu^-$  transitions [25], although the observed shift is smaller than that reported in Ref. [13]. As reported in Ref. [3], the nonlocal parameters exhibit a four-fold ambiguity that depends on the relative phases of the  $J/\psi$  and  $\psi(2S)$  amplitudes. Consequently, all four solutions for the nonlocal parameters are reported.

A fit to  $B^+ \rightarrow K^+\mu^+\mu^-$  candidates has also been performed using previous lattice QCD computations of the  $B \rightarrow K$  local form factors from the FNAL/MILC collaboration. In this case, the tension with the SM prediction of the couplings  $C_V$  and  $C_A$  is reduced to  $1.6\sigma$  owing to the larger uncertainties of the local form-factor computations.

When using HPQCD form factors, there is a mild preference for either a residual  $q^2$  dependence in  $C_A$ , or a threshold effect above the open-charm threshold in  $C_V$ . These features, although not statistically significant, may indicate missing amplitude components in the physics model or limitations in its ability to describe the data. The reconstructed dimuon mass distribution used to perform this analysis, along with the background, efficiency and resolution models, are provided in digital form in the HEPDATA page to facilitate further studies. Additional data from Run 3 of the LHC will be essential to further improve the overall accuracy and precision of the measurement.

## Acknowledgements

We express our gratitude to our colleagues in the CERN accelerator departments for the excellent performance of the LHC. We thank the technical and administrative staff at the LHCb institutes. We acknowledge support from CERN and from the national agencies: ARC (Australia); CAPES, CNPq, FAPERJ and FINEP (Brazil); MOST and NSFC (China); CNRS/IN2P3 and CEA (France); BMFTR, DFG and MPG (Germany); INFN (Italy); NWO (Netherlands); MNiSW and NCN (Poland); MCID/IFA (Romania); MICIU and AEI (Spain); SNSF and SER (Switzerland); NASU (Ukraine); STFC (United Kingdom); DOE NP and NSF (USA). We acknowledge the computing resources that are provided by ARDC (Australia), CBPF (Brazil), CERN, IHEP and LZU (China), IN2P3 (France), KIT and DESY (Germany), INFN (Italy), SURF (Netherlands), Polish WLCG (Poland), IFIN-HH (Romania), PIC (Spain), CSCS (Switzerland), GridPP (United

Kingdom), and NSF (USA). We are indebted to the communities behind the multiple open-source software packages on which we depend. Individual groups or members have received support from Key Research Program of Frontier Sciences of CAS, CAS PIFI, CAS CCEPP (China); Minciencias (Colombia); EPLANET, Marie Skłodowska-Curie Actions, ERC and NextGenerationEU (European Union); A\*MIDEX, ANR, IPhU and Labex P2IO, and Région Auvergne-Rhône-Alpes (France); Alexander-von-Humboldt Foundation (Germany); ICSC (Italy); Severo Ochoa and María de Maeztu Units of Excellence, GVA, XuntaGal, GENCAT, InTalent-Inditex and Prog. Atracción Talento CM (Spain); the Leverhulme Trust, the Royal Society and UKRI (United Kingdom).

## References

- [1] F. Mahmoudi and Y. Monceaux, *Overview of  $B \rightarrow K^{(*)}\ell\ell$ . Theoretical calculations and uncertainties*, [\*Symmetry\* \*\*16\*\* \(2024\) 1006](#), [arXiv:2408.03235](#).
- [2] M. Andersson, A. M. Marshall, K. A. Petridis, and E. Smith, *Strange Things in Bottom-to-Strange Decays: The Standard Model Turned Upside Down?*, [\*Symmetry\* \*\*16\*\* \(2024\) 638](#).
- [3] LHCb collaboration, R. Aaij *et al.*, *Measurement of the phase difference between the short- and long-distance amplitudes in the  $B^+ \rightarrow K^+\mu^+\mu^-$  decay*, [\*Eur. Phys. J.\* \*\*C77\*\* \(2017\) 161](#), [arXiv:1612.06764](#).
- [4] C. Cornella *et al.*, *Hunting for  $B^+ \rightarrow K^+\tau^+\tau^-$  imprints on the  $B^+ \rightarrow K^+\mu^+\mu^-$  dimuon spectrum*, [\*Eur. Phys. J.\* \*\*C80\*\* \(2020\) 1095](#), [arXiv:2001.04470](#).
- [5] LHCb collaboration, R. Aaij *et al.*, *A comprehensive analysis of the  $B^0 \rightarrow K^{*0}\mu^+\mu^-$  decay*, [arXiv:2512.18053](#), Submitted to *Phys. Rev. Lett.*
- [6] LHCb collaboration, R. Aaij *et al.*, *Branching fraction measurements of the rare  $B_s^0 \rightarrow \phi\mu^+\mu^-$  and  $B_s^0 \rightarrow f_2'(1525)\mu^+\mu^-$  decays*, [\*Phys. Rev. Lett.\* \*\*127\*\* \(2021\) 151801](#), [arXiv:2105.14007](#).
- [7] LHCb collaboration, R. Aaij *et al.*, *Angular analysis of the  $B^+ \rightarrow K^{*+}\mu^+\mu^-$  decay*, [\*Phys. Rev. Lett.\* \*\*126\*\* \(2021\) 161802](#), [arXiv:2012.13241](#).
- [8] LHCb collaboration, R. Aaij *et al.*, *Differential branching fractions and isospin asymmetries of  $B \rightarrow K^{(*)}\mu^+\mu^-$  decays*, [\*JHEP\* \*\*06\*\* \(2014\) 133](#), [arXiv:1403.8044](#).
- [9] CMS collaboration, A. Hayrapetyan *et al.*, *Test of lepton flavor universality in  $B^\pm \rightarrow K^\pm\mu^+\mu^-$  and  $B^\pm \rightarrow K^\pm e^+e^-$  decays in proton-proton collisions at  $\sqrt{s} = 13$  TeV*, [\*Rept. Prog. Phys.\* \*\*87\*\* \(2024\) 077802](#), [arXiv:2401.07090](#).
- [10] ATLAS collaboration, M. Aaboud *et al.*, *Angular analysis of  $B_d^0 \rightarrow K^{*0}\mu^+\mu^-$  decays in pp collisions at  $\sqrt{s} = 8$  TeV with the ATLAS detector*, [\*JHEP\* \*\*10\*\* \(2018\) 047](#), [arXiv:1805.04000](#).
- [11] Belle collaboration, S. Wehle *et al.*, *Lepton-flavor-dependent angular analysis of  $B \rightarrow K^*\ell^+\ell^-$* , [\*Phys. Rev. Lett.\* \*\*118\*\* \(2017\) 111801](#), [arXiv:1612.05014](#).

- [12] T. Hurth, F. Mahmoudi, Y. Monceaux, and S. Neshatpour, *Data-driven analyses and model-independent fits for present  $b \rightarrow s\ell\ell$  results*, *Phys. Rev.* **D112** (2025) 113003, [arXiv:2508.09986](#).
- [13] M. Bordone, G. Isidori, S. Mächler, and A. Tinari, *Short- vs. long-distance physics in  $B \rightarrow K^{(*)}\ell^+\ell^-$ : a data-driven analysis*, *Eur. Phys. J.* **C84** (2024) 547, [arXiv:2401.18007](#).
- [14] M. Algueró *et al.*, *To (b)e or not to (b)e: no electrons at LHCb*, *Eur. Phys. J.* **C83** (2023) 648, [arXiv:2304.07330](#).
- [15] N. Gubernari, M. Reboud, D. van Dyk, and J. Virto, *Improved theory predictions and global analysis of exclusive  $b \rightarrow s\mu^+\mu^-$  processes*, *JHEP* **09** (2022) 133, [arXiv:2206.03797](#).
- [16] A. Khodjamirian, T. Mannel, A. A. Pivovarov, and Y.-M. Wang, *Charm-loop effect in  $B \rightarrow K^{(*)}\ell^+\ell^-$  and  $B \rightarrow K^*\gamma$* , *JHEP* **09** (2010) 089, [arXiv:1006.4945](#).
- [17] A. Y. Korchin and V. A. Kovalchuk, *Contribution of vector resonances to the  $\bar{B}_d^0 \rightarrow \bar{K}^{*0}\mu^+\mu^-$  decay*, *Eur. Phys. J.* **C72** (2012) 2155, [arXiv:1205.3683](#).
- [18] S. Jäger and J. Martin Camalich, *On  $B \rightarrow V\ell\ell$  at small dilepton invariant mass, power corrections, and new physics*, *JHEP* **05** (2013) 043, [arXiv:1212.2263](#).
- [19] S. Descotes-Genon, J. Matias, and J. Virto, *Understanding the  $B \rightarrow K^*\mu^+\mu^-$  anomaly*, *Phys. Rev.* **D88** (2013) 074002, [arXiv:1307.5683](#).
- [20] J. Lyon and R. Zwicky, *Resonances gone topsy turvy - the charm of QCD or new physics in  $b \rightarrow s\ell^+\ell^-$ ?*, [arXiv:1406.0566](#).
- [21] S. Jäger and J. Martin Camalich, *Reassessing the discovery potential of the  $B \rightarrow K^*\ell^+\ell^-$  decays in the large-recoil region: SM challenges and BSM opportunities*, *Phys. Rev.* **D93** (2016) 014028, [arXiv:1412.3183](#).
- [22] M. Ciuchini *et al.*,  *$B \rightarrow K^*\ell^+\ell^-$  decays at large recoil in the Standard Model: a theoretical reappraisal*, *JHEP* **06** (2016) 116, [arXiv:1512.07157](#).
- [23] N. Gubernari, D. van Dyk, and J. Virto, *Non-local matrix elements in  $B_{(s)} \rightarrow \{K^{(*)}, \phi\}\ell^+\ell^-$* , *JHEP* **02** (2021) 088, [arXiv:2011.09813](#).
- [24] M. Ciuchini *et al.*, *Constraints on lepton universality violation from rare  $B$  decays*, *Phys. Rev.* **D107** (2023) 055036, [arXiv:2212.10516](#).
- [25] N. Gubernari, M. Reboud, D. van Dyk, and J. Virto, *Improved theory predictions and global analysis of exclusive  $b \rightarrow s\mu^+\mu^-$  processes*, *JHEP* **09** (2022) 133, [arXiv:2206.03797](#).
- [26] G. Isidori, Z. Polonsky, and A. Tinari, *Explicit estimate of charm rescattering in  $B^0 \rightarrow K^0\bar{\ell}\ell$* , *Phys. Rev. D* **111** (2025) 093007, [arXiv:2405.17551](#).
- [27] G. Isidori, Z. Polonsky, and A. Tinari, *Charm rescattering in  $B^0 \rightarrow K^0\bar{\ell}\ell$ : an improved analysis*, *Eur. Phys. J. C* **85** (2025) 1221, [arXiv:2507.17824](#).

- [28] LHCb collaboration, R. Aaij *et al.*, *Comprehensive analysis of local and nonlocal amplitudes in the  $B^0 \rightarrow K^{*0}\mu^+\mu^-$  decay*, *JHEP* **09** (2024) 026, [arXiv:2405.17347](#).
- [29] LHCb collaboration, R. Aaij *et al.*, *Amplitude analysis of the  $B^0 \rightarrow K^*(892)^0\mu^+\mu^-$  decay*, *Phys. Rev. Lett.* **132** (2024) 131801, [arXiv:2312.09115](#).
- [30] Particle Data Group, S. Navas *et al.*, *Review of particle physics*, *Phys. Rev.* **D110** (2024) 030001.
- [31] S. M. Flatté, *Coupled-channel analysis of the  $\pi\eta$  and  $K\bar{K}$  systems near  $K\bar{K}$  threshold*, *Phys. Lett.* **B63** (1976) 224.
- [32] BaBar collaboration, J. P. Lees *et al.*, *Precision measurement of the  $e^+e^- \rightarrow K^+K^-(\gamma)$  cross section with the initial-state radiation method at BABAR*, *Phys. Rev.* **D88** (2013) 032013, [arXiv:1306.3600](#).
- [33] E. A. Kozyrev *et al.*, *Study of the process  $e^+e^- \rightarrow K^+K^-$  in the center-of-mass energy range 1010–1060 MeV with the CMD-3 detector*, *Phys. Lett.* **B779** (2018) 64, [arXiv:1710.02989](#).
- [34] LHCb collaboration, R. Aaij *et al.*, *Measurement of CP asymmetries in the decays  $B^0 \rightarrow K^*(892)^0\mu^+\mu^-$  and  $B^+ \rightarrow K^+\mu^+\mu^-$* , *JHEP* **09** (2014) 177, [arXiv:1408.0978](#).
- [35] A. K. Alok *et al.*, *New physics in  $b \rightarrow s\mu^+\mu^-$ : CP-violating observables*, *JHEP* **11** (2011) 122, [arXiv:1103.5344](#).
- [36] HPQCD collaboration, W. G. Parrott, C. Bouchard, and C. T. H. Davies,  *$B \rightarrow K$  and  $D \rightarrow K$  form factors from fully relativistic lattice QCD*, *Phys. Rev.* **D107** (2023) 014510, [arXiv:2207.12468](#).
- [37] FNAL/MILC collaboration, J. A. Bailey *et al.*,  *$B \rightarrow K\ell^+\ell^-$  decay form factors from three-flavor lattice QCD*, *Phys. Rev.* **D93** (2016) 025026, [arXiv:1509.06235](#).
- [38] LHCb collaboration, A. A. Alves Jr. *et al.*, *The LHCb detector at the LHC*, *JINST* **3** (2008) S08005.
- [39] LHCb collaboration, R. Aaij *et al.*, *LHCb detector performance*, *Int. J. Mod. Phys.* **A30** (2015) 1530022, [arXiv:1412.6352](#).
- [40] A. A. Alves Jr. *et al.*, *Performance of the LHCb muon system*, *JINST* **8** (2013) P02022, [arXiv:1211.1346](#).
- [41] N. Grieser *et al.*, *The LHCb stripping project: Sustainable legacy data processing for high-energy physics*, *Comput. Softw. Big. Sci.* **9** (2025) 21, [arXiv:2509.05294](#).
- [42] T. Sjöstrand, S. Mrenna, and P. Skands, *A brief introduction to PYTHIA 8.1*, *Comput. Phys. Commun.* **178** (2008) 852, [arXiv:0710.3820](#).
- [43] I. Belyaev *et al.*, *Handling of the generation of primary events in Gauss, the LHCb simulation framework*, *J. Phys. Conf. Ser.* **331** (2011) 032047.
- [44] D. J. Lange, *The EvtGen particle decay simulation package*, *Nucl. Instrum. Meth.* **A462** (2001) 152.

- [45] N. Davidson, T. Przedzinski, and Z. Was, *PHOTOS interface in C++: Technical and physics documentation*, *Comput. Phys. Commun.* **199** (2016) 86, [arXiv:1011.0937](#).
- [46] Geant4 collaboration, J. Allison *et al.*, *Geant4 developments and applications*, *IEEE Trans. Nucl. Sci.* **53** (2006) 270; Geant4 collaboration, S. Agostinelli *et al.*, *Geant4: A simulation toolkit*, *Nucl. Instrum. Meth.* **A506** (2003) 250.
- [47] M. Clemencic *et al.*, *The LHCb simulation application, Gauss: Design, evolution and experience*, *J. Phys. Conf. Ser.* **331** (2011) 032023.
- [48] L. Breiman, J. Friedman, C. J. Stone, and R. A. Olshen, *Classification and regression trees*, *Chapman and Hall/CRC*, 1984.
- [49] Y. Freund and R. E. Schapire, *A decision-theoretic generalization of on-line learning and an application to boosting*, *Journ. of Comp. and Sys. Sci.* **55** (1997) 119.
- [50] A. Blum, A. Kalai, and J. Langford, *Beating the hold-out: bounds for k-fold and progressive cross-validation*, in *Proceedings of the Twelfth Annual Conference on Computational Learning Theory, COLT '99*, (New York, NY, USA), 203208, *Association for Computing Machinery*, 1999.
- [51] C. Bobeth, G. Hiller, and G. Piranishvili, *Angular distributions of  $\bar{B} \rightarrow \bar{K}\ell^+\ell^-$  decays*, *JHEP* **12** (2007) 040, [arXiv:0709.4174](#).
- [52] T. Skwarnicki, *A study of the radiative cascade transitions between the Upsilon-prime and Upsilon resonances*, PhD thesis, Institute of Nuclear Physics, Krakow, 1986, [DESY-F31-86-02](#).
- [53] K. S. Cranmer, *Kernel estimation in high-energy physics*, *Comput. Phys. Commun.* **136** (2001) 198, [arXiv:hep-ex/0011057](#).
- [54] ARGUS collaboration, H. Albrecht *et al.*, *Measurement of the polarization in the decay  $B \rightarrow J/\psi K^*$* , *Phys. Lett.* **B340** (1994) 217.
- [55] BES collaboration, M. Ablikim *et al.*, *Determination of the  $\psi(3770)$ ,  $\psi(4040)$ ,  $\psi(4160)$  and  $\psi(4415)$  resonance parameters*, *Phys. Lett.* **B660** (2008) 315, [arXiv:0705.4500](#).
- [56] M. Jung, *Branching ratio measurements and isospin violation in B-meson decays*, *Phys. Lett.* **B753** (2016) 187, [arXiv:1510.03423](#).

## LHCb collaboration

R. Aaij<sup>38</sup> , A.S.W. Abdelmotteleb<sup>58</sup> , C. Abellan Beteta<sup>52</sup> , F. Abudinén<sup>60</sup> ,  
T. Ackernley<sup>62</sup> , A. A. Adefisoye<sup>70</sup> , B. Adeva<sup>48</sup> , M. Adinolfi<sup>56</sup> , P. Adlarson<sup>86</sup> ,  
C. Agapopoulou<sup>14</sup> , C.A. Aidala<sup>88</sup> , Z. Ajaltouni<sup>11</sup> , S. Akar<sup>11</sup> , K. Akiba<sup>38</sup> ,  
P. Albicocco<sup>28</sup> , J. Albrecht<sup>19,g</sup> , R. Aleksiejunas<sup>82</sup> , F. Alessio<sup>50</sup> ,  
P. Alvarez Cartelle<sup>57,48</sup> , R. Amalric<sup>16</sup> , S. Amato<sup>3</sup> , J.L. Amey<sup>56</sup> , Y. Amhis<sup>14</sup> ,  
L. An<sup>6</sup> , L. Anderlini<sup>27</sup> , M. Andersson<sup>52</sup> , P. Andreola<sup>52</sup> , M. Andreotti<sup>26</sup> , S.  
Andres Estrada<sup>45</sup> , A. Anelli<sup>31,p</sup> , D. Ao<sup>7</sup> , C. Arata<sup>12</sup> , F. Archilli<sup>37</sup> , Z. Areg<sup>70</sup> ,  
M. Argenton<sup>26</sup> , S. Arguedas Cuendis<sup>9,50</sup> , L. Arnone<sup>31,p</sup> , A. Artamonov<sup>44</sup> ,  
M. Artuso<sup>70</sup> , E. Aslanides<sup>13</sup> , R. Ataíde Da Silva<sup>51</sup> , M. Atzeni<sup>66</sup> , B. Audurier<sup>12</sup> , J.  
A. Authier<sup>15</sup> , D. Bacher<sup>65</sup> , I. Bachiller Perea<sup>51</sup> , S. Bachmann<sup>22</sup> , M. Bachmayer<sup>51</sup> ,  
J.J. Back<sup>58</sup> , P. Baladron Rodriguez<sup>48</sup> , V. Balagura<sup>15</sup> , A. Balboni<sup>26</sup> , W. Baldini<sup>26</sup> ,  
Z. Baldwin<sup>80</sup> , L. Balzani<sup>19</sup> , H. Bao<sup>7</sup> , J. Baptista de Souza Leite<sup>2</sup> ,  
C. Barbero Pretel<sup>48,12</sup> , M. Barbetti<sup>27</sup> , I. R. Barbosa<sup>71</sup> , R.J. Barlow<sup>64,†</sup> ,  
M. Barnyakov<sup>25</sup> , S. Barsuk<sup>14</sup> , W. Barter<sup>60</sup> , J. Bartz<sup>70</sup> , S. Bashir<sup>40</sup> , B. Batsukh<sup>5</sup> ,  
P. B. Battista<sup>14</sup> , A. Bavarchee<sup>81</sup> , A. Bay<sup>51</sup> , A. Beck<sup>66</sup> , M. Becker<sup>19</sup> ,  
F. Bedeschi<sup>35</sup> , I.B. Bediaga<sup>2</sup> , N. A. Behling<sup>19</sup> , S. Belin<sup>48</sup> , A. Bellavista<sup>25</sup> ,  
K. Belous<sup>44</sup> , I. Belov<sup>29</sup> , I. Belyaev<sup>36</sup> , G. Benane<sup>13</sup> , G. Bencivenni<sup>28</sup> ,  
E. Ben-Haim<sup>16</sup> , A. Berezhnoy<sup>44</sup> , R. Bernet<sup>52</sup> , S. Bernet Andres<sup>47</sup> , A. Bertolin<sup>33</sup> ,  
F. Betti<sup>60</sup> , J. Bex<sup>57</sup> , O. Bezshyyko<sup>87</sup> , S. Bhattacharya<sup>81</sup> , M.S. Bieker<sup>18</sup> ,  
N.V. Biesuz<sup>26</sup> , A. Biolchini<sup>38</sup> , M. Birch<sup>63</sup> , F.C.R. Bishop<sup>10</sup> , A. Bitadze<sup>64</sup> ,  
A. Bizzeti<sup>27,g</sup> , T. Blake<sup>58,c</sup> , F. Blanc<sup>51</sup> , J.E. Blank<sup>19</sup> , S. Blusk<sup>70</sup> ,  
V. Bocharnikov<sup>44</sup> , J.A. Boelhauve<sup>19</sup> , O. Boente Garcia<sup>50</sup> , T. Boettcher<sup>69</sup> , A.  
Bohare<sup>60</sup> , A. Boldyrev<sup>44</sup> , C. Bolognani<sup>84</sup> , R. Bolzonella<sup>26,m</sup> , R. B. Bonacci<sup>1</sup> ,  
N. Bondar<sup>44,50</sup> , A. Bordelius<sup>50</sup> , F. Borgato<sup>33,50</sup> , S. Borghi<sup>64</sup> , M. Borsato<sup>31,p</sup> ,  
J.T. Borsuk<sup>85</sup> , E. Bottalico<sup>62</sup> , S.A. Bouchiba<sup>51</sup> , M. Bovill<sup>65</sup> , T.J.V. Bowcock<sup>62</sup> ,  
A. Boyer<sup>50</sup> , C. Bozzi<sup>26</sup> , J. D. Brandenburg<sup>89</sup> , A. Brea Rodriguez<sup>51</sup> , N. Breer<sup>19</sup> ,  
J. Brodzicka<sup>41</sup> , J. Brown<sup>62</sup> , D. Brundu<sup>32</sup> , E. Buchanan<sup>60</sup> , M. Burgos Marcos<sup>84</sup> ,  
A.T. Burke<sup>64</sup> , C. Burr<sup>50</sup> , C. Buti<sup>27</sup> , J.S. Butter<sup>57</sup> , J. Buytaert<sup>50</sup> ,  
W. Byczynski<sup>50</sup> , S. Cadeddu<sup>32</sup> , H. Cai<sup>76</sup> , Y. Cai<sup>5</sup> , A. Caillet<sup>16</sup> ,  
R. Calabrese<sup>26,m</sup> , S. Calderon Ramirez<sup>9</sup> , L. Calefice<sup>46</sup> , M. Calvi<sup>31,p</sup> ,  
M. Calvo Gomez<sup>47</sup> , P. Camargo Magalhaes<sup>2,a</sup> , J. I. Cambon Bouzas<sup>48</sup> , P. Campana<sup>28</sup> ,  
A. C. Campos<sup>3</sup> , A.F. Campoverde Quezada<sup>7</sup> , Y. Cao<sup>6</sup> , S. Capelli<sup>31</sup> , M. Caporale<sup>25</sup> ,  
L. Capriotti<sup>26</sup> , R. Caravaca-Mora<sup>9</sup> , A. Carbone<sup>25,k</sup> , L. Carcedo Salgado<sup>48</sup> ,  
R. Cardinale<sup>29,n</sup> , A. Cardini<sup>32</sup> , P. Carniti<sup>31</sup> , L. Carus<sup>22</sup> , A. Casais Vidal<sup>66</sup> ,  
R. Caspary<sup>22</sup> , G. Casse<sup>62</sup> , M. Cattaneo<sup>50</sup> , G. Cavallero<sup>26</sup> , V. Cavallini<sup>26,m</sup> ,  
S. Celani<sup>50</sup> , I. Celestino<sup>35,t</sup> , S. Cesare<sup>50,o</sup> , A.J. Chadwick<sup>62</sup> , I. Chahrour<sup>88</sup> , H.  
Chang<sup>4,d</sup> , M. Charles<sup>16</sup> , Ph. Charpentier<sup>50</sup> , E. Chatzianagnostou<sup>38</sup> , R. Cheaib<sup>81</sup> ,  
M. Chefdeville<sup>10</sup> , C. Chen<sup>57</sup> , J. Chen<sup>51</sup> , S. Chen<sup>5</sup> , Z. Chen<sup>7</sup> , A. Chen Hu<sup>63</sup> , M.  
Cherif<sup>12</sup> , A. Chernov<sup>41</sup> , S. Chernyshenko<sup>54</sup> , X. Chiotopoulos<sup>84</sup> , V. Chobanova<sup>45</sup> ,  
M. Chrzaszcz<sup>41</sup> , A. Chubykin<sup>44</sup> , V. Chulikov<sup>28,36,50</sup> , P. Ciambone<sup>28</sup> ,  
X. Cid Vidal<sup>48</sup> , G. Ciezarek<sup>50</sup> , P. Cifra<sup>50</sup> , P.E.L. Clarke<sup>60</sup> , M. Clemencic<sup>50</sup> ,  
H.V. Cliff<sup>57</sup> , J. Closier<sup>50</sup> , C. Cocha Toapaxi<sup>22</sup> , V. Coco<sup>50</sup> , J. Cogan<sup>13</sup> ,  
E. Cogneras<sup>11</sup> , L. Cojocariu<sup>43</sup> , S. Collaviti<sup>51</sup> , P. Collins<sup>50</sup> , T. Colombo<sup>50</sup> ,  
M. Colonna<sup>19</sup> , A. Comerma-Montells<sup>46</sup> , L. Congedo<sup>24</sup> , J. Connaughton<sup>58</sup> ,  
A. Contu<sup>32</sup> , N. Cooke<sup>61</sup> , G. Cordova<sup>35,t</sup> , C. Coronel<sup>67</sup> , I. Corredoira<sup>12</sup> ,  
A. Correia<sup>16</sup> , G. Corti<sup>50</sup> , J. Cottee Meldrum<sup>56</sup> , B. Couturier<sup>50</sup> , D.C. Craik<sup>52</sup> ,  
M. Cruz Torres<sup>2,h</sup> , M. Cubero Campos<sup>9</sup> , E. Curras Rivera<sup>51</sup> , R. Currie<sup>60</sup> ,  
C.L. Da Silva<sup>69</sup> , S. Dadabaev<sup>44</sup> , X. Dai<sup>4</sup> , E. Dall’Occo<sup>50</sup> , J. Dalseno<sup>45</sup> 

C. D'Ambrosio<sup>63</sup> , J. Daniel<sup>11</sup> , G. Darze<sup>3</sup> , A. Davidson<sup>58</sup> , J.E. Davies<sup>64</sup> ,  
 O. De Aguiar Francisco<sup>64</sup> , C. De Angelis<sup>32,l</sup> , F. De Benedetti<sup>50</sup> , J. de Boer<sup>38</sup> ,  
 K. De Bruyn<sup>83</sup> , S. De Capua<sup>64</sup> , M. De Cian<sup>64,50</sup> , U. De Freitas Carneiro Da Graca<sup>2,b</sup> ,  
 E. De Lucia<sup>28</sup> , J.M. De Miranda<sup>2</sup> , L. De Paula<sup>3</sup> , M. De Serio<sup>24,i</sup> , P. De Simone<sup>28</sup> ,  
 F. De Vellis<sup>19</sup> , J.A. de Vries<sup>84</sup> , F. Debernardis<sup>24</sup> , D. Decamp<sup>10</sup> , S. Dekkers<sup>1</sup> ,  
 L. Del Buono<sup>16</sup> , B. Delaney<sup>66</sup> , J. Deng<sup>8</sup> , V. Denysenko<sup>52</sup> , O. Deschamps<sup>11</sup> ,  
 F. Dettori<sup>32,l</sup> , B. Dey<sup>81</sup> , P. Di Nezza<sup>28</sup> , I. Diachkov<sup>44</sup> , S. Didenko<sup>44</sup> , S. Ding<sup>70</sup> ,  
 Y. Ding<sup>51</sup> , L. Dittmann<sup>22</sup> , V. Dobishuk<sup>54</sup> , A. D. Docheva<sup>61</sup> , A. Doheny<sup>58</sup> ,  
 C. Dong<sup>d,4</sup> , A.M. Donohoe<sup>23</sup> , F. Dordei<sup>32</sup> , A.C. dos Reis<sup>2</sup> , A. D. Dowling<sup>70</sup> ,  
 L. Dreyfus<sup>13</sup> , W. Duan<sup>74</sup> , P. Duda<sup>85</sup> , L. Dufour<sup>51</sup> , V. Duk<sup>34</sup> , P. Durante<sup>50</sup> , M.  
 M. Duras<sup>85</sup> , J.M. Durham<sup>69</sup> , O. D. Durmus<sup>81</sup> , A. Dziurda<sup>41</sup> , A. Dzyuba<sup>44</sup> ,  
 S. Easo<sup>59</sup> , E. Eckstein<sup>18</sup> , U. Egede<sup>1</sup> , A. Egorychev<sup>44</sup> , V. Egorychev<sup>44</sup> ,  
 S. Eisenhardt<sup>60</sup> , E. Ejopu<sup>62</sup> , L. Eklund<sup>86</sup> , M. Elashri<sup>67</sup> , D. Elizondo Blanco<sup>9</sup> ,  
 J. Ellbracht<sup>19</sup> , S. Ely<sup>63</sup> , A. Ene<sup>43</sup> , J. Eschle<sup>70</sup> , T. Evans<sup>38</sup> , F. Fabiano<sup>14</sup> , S.  
 Faghil<sup>67</sup> , L.N. Falcao<sup>31,p</sup> , B. Fang<sup>7</sup> , R. Fantechi<sup>35</sup> , L. Fantini<sup>34,s</sup> , M. Faria<sup>51</sup> , K.  
 Farmer<sup>60</sup> , F. Fassin<sup>83,38</sup> , D. Fazzini<sup>31,p</sup> , L. Felkowski<sup>85</sup> , C. Feng<sup>6</sup> , M. Feng<sup>5,7</sup> ,  
 A. Fernandez Casani<sup>49</sup> , M. Fernandez Gomez<sup>48</sup> , A.D. Fernez<sup>68</sup> , F. Ferrari<sup>25,k</sup> ,  
 F. Ferreira Rodrigues<sup>3</sup> , M. Ferrillo<sup>52</sup> , M. Ferro-Luzzi<sup>50</sup> , S. Filippov<sup>44</sup> , R.A. Fini<sup>24</sup> ,  
 M. Fiorini<sup>26,m</sup> , M. Firlej<sup>40</sup> , K.L. Fischer<sup>65</sup> , D.S. Fitzgerald<sup>88</sup> , C. Fitzpatrick<sup>64</sup> ,  
 T. Fiutowski<sup>40</sup> , F. Fleuret<sup>15</sup> , A. Fomin<sup>53</sup> , M. Fontana<sup>25,50</sup> , L. A. Foreman<sup>64</sup> ,  
 R. Forty<sup>50</sup> , D. Foulds-Holt<sup>60</sup> , V. Franco Lima<sup>3</sup> , M. Franco Sevilla<sup>68</sup> , M. Frank<sup>50</sup> ,  
 E. Franzoso<sup>26,m</sup> , G. Frau<sup>64</sup> , C. Frei<sup>50</sup> , D.A. Friday<sup>64,50</sup> , J. Fu<sup>7</sup> , Q. Führung<sup>19,g,57</sup> ,  
 T. Fulghesu<sup>13</sup> , G. Galati<sup>24,i</sup> , M.D. Galati<sup>38</sup> , A. Gallas Torreira<sup>48</sup> , D. Galli<sup>25,k</sup> ,  
 S. Gambetta<sup>60</sup> , M. Gandelman<sup>3</sup> , P. Gandini<sup>30</sup> , B. Ganie<sup>64</sup> , H. Gao<sup>7</sup> , R. Gao<sup>65</sup> ,  
 T.Q. Gao<sup>57</sup> , Y. Gao<sup>8</sup> , Y. Gao<sup>6</sup> , Y. Gao<sup>8</sup> , L.M. Garcia Martin<sup>51</sup> ,  
 P. Garcia Moreno<sup>46</sup> , J. García Pardiñas<sup>66</sup> , P. Gardner<sup>68</sup> , L. Garrido<sup>46</sup> ,  
 C. Gaspar<sup>50</sup> , A. Gavrikov<sup>33</sup> , L.L. Gerken<sup>19</sup> , E. Gersabeck<sup>20</sup> , M. Gersabeck<sup>20</sup> ,  
 T. Gershon<sup>58</sup> , S. Ghizzo<sup>29,n</sup> , Z. Ghorbanimoghaddam<sup>56</sup> , F. I. Giasemis<sup>16,f</sup> ,  
 V. Gibson<sup>57</sup> , H.K. Gienza<sup>42</sup> , A.L. Gilman<sup>67</sup> , M. Giovannetti<sup>28</sup> , A. Gioventù<sup>46</sup> ,  
 L. Girardey<sup>64,59</sup> , M.A. Giza<sup>41</sup> , F.C. Glaser<sup>22,14</sup> , V.V. Gligorov<sup>16</sup> , C. Göbel<sup>71</sup> , L.  
 Golinka-Bezshyyko<sup>87</sup> , E. Golobardes<sup>47</sup> , D. Golubkov<sup>44</sup> , A. Golutvin<sup>63,50</sup> ,  
 S. Gomez Fernandez<sup>46</sup> , W. Gomulka<sup>40</sup> , F. Goncalves Abrantes<sup>65</sup> , I. Gonçales Vaz<sup>50</sup> ,  
 M. Goncerz<sup>41</sup> , G. Gong<sup>4,d</sup> , J. A. Gooding<sup>19</sup> , I.V. Gorelov<sup>44</sup> , C. Gottl<sup>31</sup> ,  
 E. Govorkova<sup>66</sup> , J.P. Grabowski<sup>30</sup> , L.A. Granado Cardoso<sup>50</sup> , E. Graugés<sup>46</sup> ,  
 E. Graverini<sup>35,51</sup> , L. Grazette<sup>58</sup> , G. Graziani<sup>27</sup> , A. T. Grecu<sup>43</sup> , N.A. Grieser<sup>67</sup> ,  
 L. Grillo<sup>61</sup> , S. Gromov<sup>44</sup> , C. Gu<sup>15</sup> , M. Guarise<sup>26</sup> , L. Guerry<sup>11</sup> ,  
 A.-K. Guseinov<sup>51</sup> , E. Gushchin<sup>44</sup> , Y. Guz<sup>6,50</sup> , T. Gys<sup>50</sup> , K. Habermann<sup>18</sup> ,  
 T. Hadavizadeh<sup>1</sup> , C. Hadjivasiliou<sup>68</sup> , G. Haefeli<sup>51</sup> , C. Haen<sup>50</sup> , S. Haken<sup>57</sup> , G.  
 Hallett<sup>58</sup> , P.M. Hamilton<sup>68</sup> , J. Hammerich<sup>62</sup> , Q. Han<sup>33</sup> , X. Han<sup>22,50</sup> ,  
 S. Hansmann-Menzemer<sup>22</sup> , L. Hao<sup>7</sup> , N. Harnew<sup>65</sup> , T. J. Harris<sup>1</sup> , M. Hartmann<sup>14</sup> ,  
 S. Hashmi<sup>40</sup> , J. He<sup>7,e</sup> , N. Heatley<sup>14</sup> , A. Hedes<sup>64</sup> , F. Hemmer<sup>50</sup> , C. Henderson<sup>67</sup> ,  
 R. Henderson<sup>14</sup> , R.D.L. Henderson<sup>1</sup> , A.M. Hennequin<sup>50</sup> , K. Hennessy<sup>62</sup> ,  
 L. Henry<sup>51</sup> , J. Herd<sup>63</sup> , P. Herrero Gascon<sup>22</sup> , J. Heuel<sup>17</sup> , A. Heyn<sup>13</sup> , A. Hicheur<sup>3</sup> ,  
 G. Hijano Mendizabal<sup>52</sup> , J. Horswill<sup>64</sup> , R. Hou<sup>8</sup> , Y. Hou<sup>11</sup> , D.C. Houston<sup>61</sup> ,  
 N. Howarth<sup>62</sup> , W. Hu<sup>7</sup> , X. Hu<sup>4</sup> , W. Hulsbergen<sup>38</sup> , R.J. Hunter<sup>58</sup> ,  
 M. Hushchyn<sup>44</sup> , D. Hutchcroft<sup>62</sup> , M. Idzik<sup>40</sup> , D. Ilin<sup>44</sup> , P. Ilten<sup>67</sup> , A. Iniukhin<sup>44</sup> ,  
 A. Iohner<sup>10</sup> , A. Ishteev<sup>44</sup> , K. Ivshin<sup>44</sup> , H. Jage<sup>17</sup> , S.J. Jaimes Elles<sup>78,49,50</sup> ,  
 S. Jakobsen<sup>50</sup> , T. Jakoubek<sup>79</sup> , E. Jans<sup>38</sup> , B.K. Jashal<sup>49</sup> , A. Jawahery<sup>68</sup> , C.  
 Jayaweera<sup>55</sup> , A. Jelavic<sup>1</sup> , V. Jevtic<sup>19</sup> , Z. Jia<sup>16</sup> , E. Jiang<sup>68</sup> , X. Jiang<sup>5,7</sup> ,  
 Y. Jiang<sup>7</sup> , Y. J. Jiang<sup>6</sup> , E. Jimenez Moya<sup>9</sup> , N. Jindal<sup>89</sup> , M. John<sup>65</sup> , A.

John Rubesh Rajan<sup>23</sup> , D. Johnson<sup>55</sup> , C.R. Jones<sup>57</sup> , S. Joshi<sup>42</sup> , B. Jost<sup>50</sup> , J. Juan Castella<sup>57</sup> , N. Jurik<sup>50</sup> , I. Juszczak<sup>41</sup> , K. Kalecinska<sup>40</sup> , D. Kaminaris<sup>51</sup> , S. Kandybei<sup>53</sup> , M. Kane<sup>60</sup> , Y. Kang<sup>4,d</sup> , C. Kar<sup>11</sup> , M. Karacson<sup>50</sup> , A. Kauniskangas<sup>51</sup> , J.W. Kautz<sup>67</sup> , M.K. Kazanecki<sup>41</sup> , F. Keizer<sup>50</sup> , M. Kenzie<sup>57</sup> , T. Ketel<sup>38</sup> , B. Khanji<sup>70</sup> , A. Kharisova<sup>44</sup> , S. Kholodenko<sup>63,50</sup> , G. Khreich<sup>14</sup> , F. Kiraz<sup>14</sup> , T. Kirn<sup>17</sup> , V.S. Kirsebom<sup>31,p</sup> , S. Klaver<sup>39</sup> , N. Kleijne<sup>35,t</sup> , A. Kleimenova<sup>51</sup> , D. K. Klekots<sup>87</sup> , K. Klimaszewski<sup>42</sup> , M.R. Kmiec<sup>42</sup> , T. Knospe<sup>19</sup> , R. Kolb<sup>22</sup> , S. Koliiev<sup>54</sup> , L. Kolk<sup>19</sup> , A. Konoplyannikov<sup>6</sup> , P. Kopciwicz<sup>50</sup> , P. Koppenburg<sup>38</sup> , A. Korchin<sup>53</sup> , I. Kostiuk<sup>38</sup> , O. Kot<sup>54</sup> , S. Kotriakhova , E. Kowalczyk<sup>68</sup> , A. Kozachuk<sup>44</sup> , P. Kravchenko<sup>44</sup> , L. Kravchuk<sup>44</sup> , O. Kravcov<sup>82</sup> , M. Kreps<sup>58</sup> , P. Krokovny<sup>44</sup> , W. Krupa<sup>70</sup> , W. Krzemien<sup>42</sup> , O. Kshyvanskyi<sup>54</sup> , S. Kubis<sup>85</sup> , M. Kucharczyk<sup>41</sup> , V. Kudryavtsev<sup>44</sup> , E. Kulikova<sup>44</sup> , A. Kupsc<sup>86</sup> , V. Kushnir<sup>53</sup> , B. Kutsenko<sup>13</sup> , J. Kvapil<sup>69</sup> , I. Kyryllin<sup>53</sup> , D. Lacarrere<sup>50</sup> , P. Laguarda Gonzalez<sup>46</sup> , A. Lai<sup>32</sup> , A. Lampis<sup>32</sup> , D. Lancierini<sup>63</sup> , C. Landesa Gomez<sup>48</sup> , J.J. Lane<sup>1</sup> , G. Lanfranchi<sup>28</sup> , C. Langenbruch<sup>22</sup> , J. Langer<sup>19</sup> , T. Latham<sup>58</sup> , F. Lazzari<sup>35,u</sup> , C. Lazzeroni<sup>55</sup> , R. Le Gac<sup>13</sup> , H. Lee<sup>62</sup> , R. Lefèvre<sup>11</sup> , A. Leflat<sup>44</sup> , S. Legotin<sup>44</sup> , M. Lehuraux<sup>58</sup> , E. Lemos Cid<sup>50</sup> , O. Leroy<sup>13</sup> , T. Lesiak<sup>41</sup> , E. D. Lesser<sup>50</sup> , B. Leverington<sup>22</sup> , A. Li<sup>4,d</sup> , C. Li<sup>4</sup> , C. Li<sup>13</sup> , H. Li<sup>74</sup> , J. Li<sup>8</sup> , K. Li<sup>77</sup> , L. Li<sup>64</sup> , M. Li<sup>8</sup> , P. Li<sup>7</sup> , P.-R. Li<sup>75</sup> , Q. Li<sup>5,7</sup> , T. Li<sup>73</sup> , T. Li<sup>74</sup> , Y. Li<sup>8</sup> , Y. Li<sup>5</sup> , Y. Li<sup>4</sup> , Z. Lian<sup>4,d</sup> , Q. Liang<sup>8</sup> , X. Liang<sup>70</sup> , Z. Liang<sup>32</sup> , S. Libralon<sup>49</sup> , A. Lightbody<sup>12</sup> , C. Lin<sup>7</sup> , T. Lin<sup>59</sup> , R. Lindner<sup>50</sup> , H. Linton<sup>63</sup> , R. Litvinov<sup>32</sup> , D. Liu<sup>8</sup> , F. L. Liu<sup>1</sup> , G. Liu<sup>74</sup> , K. Liu<sup>75</sup> , S. Liu<sup>5</sup> , W. Liu<sup>8</sup> , Y. Liu<sup>60</sup> , Y. Liu<sup>75</sup> , Y. L. Liu<sup>63</sup> , G. Loachamin Ordenez<sup>71</sup> , I. Lobo<sup>1</sup> , A. Lobo Salvia<sup>10</sup> , A. Loi<sup>32</sup> , T. Long<sup>57</sup> , F. C. L. Lopes<sup>2,a</sup> , J.H. Lopes<sup>3</sup> , A. Lopez Huertas<sup>46</sup> , C. Lopez Iribarnegaray<sup>48</sup> , S. López Soliño<sup>48</sup> , Q. Lu<sup>15</sup> , C. Lucarelli<sup>50</sup> , D. Lucchesi<sup>33,r</sup> , M. Lucio Martinez<sup>49</sup> , Y. Luo<sup>6</sup> , A. Lupato<sup>33,j</sup> , E. Luppi<sup>26,m</sup> , K. Lynch<sup>23</sup> , S. Lyu<sup>6</sup> , X.-R. Lyu<sup>7</sup> , G. M. Ma<sup>4,d</sup> , H. Ma<sup>73</sup> , S. Maccolini<sup>19</sup> , F. Machefert<sup>14</sup> , F. Maciuc<sup>43</sup> , B. Mack<sup>70</sup> , I. Mackay<sup>65</sup> , L. M. Mackey<sup>70</sup> , L.R. Madhan Mohan<sup>57</sup> , M. J. Madurai<sup>55</sup> , D. Magdalinski<sup>38</sup> , D. Maisuzenko<sup>44</sup> , J.J. Malczewski<sup>41</sup> , S. Malde<sup>65</sup> , L. Malentacca<sup>50</sup> , A. Malinin<sup>44</sup> , T. Maltsev<sup>44</sup> , G. Manca<sup>32,l</sup> , G. Mancinelli<sup>13</sup> , C. Mancuso<sup>14</sup> , R. Manera Escalero<sup>46</sup> , F. M. Manganella<sup>37</sup> , D. Manuzzi<sup>25</sup> , D. Marangotto<sup>30,o</sup> , J.F. Marchand<sup>10</sup> , R. Marchevski<sup>51</sup> , U. Marconi<sup>25</sup> , E. Mariani<sup>16</sup> , S. Mariani<sup>50</sup> , C. Marin Benito<sup>46</sup> , J. Marks<sup>22</sup> , A.M. Marshall<sup>56</sup> , L. Martel<sup>65</sup> , G. Martelli<sup>34</sup> , G. Martellotti<sup>36</sup> , L. Martinazzoli<sup>50</sup> , M. Martinelli<sup>31,p</sup> , D. Martinez Gomez<sup>83</sup> , D. Martinez Santos<sup>45</sup> , F. Martinez Vidal<sup>49</sup> , A. Martorell i Granollers<sup>47</sup> , A. Massafferri<sup>2</sup> , R. Matev<sup>50</sup> , A. Mathad<sup>50</sup> , V. Matiunin<sup>44</sup> , C. Matteuzzi<sup>70</sup> , K.R. Mattioli<sup>15</sup> , A. Mauri<sup>63</sup> , E. Maurice<sup>15</sup> , J. Mauricio<sup>46</sup> , P. Mayencourt<sup>51</sup> , J. Mazorra de Cos<sup>49</sup> , M. Mazurek<sup>42</sup> , D. Mazzanti Tarancon<sup>46</sup> , M. McCann<sup>63</sup> , N.T. McHugh<sup>61</sup> , A. McNab<sup>64</sup> , R. McNulty<sup>23</sup> , B. Meadows<sup>67</sup> , D. Melnychuk<sup>42</sup> , D. Mendoza Granada<sup>16</sup> , P. Menendez Valdes Perez<sup>48</sup> , F. M. Meng<sup>4,d</sup> , M. Merk<sup>38,84</sup> , A. Merli<sup>51,30</sup> , L. Meyer Garcia<sup>68</sup> , D. Miao<sup>5,7</sup> , H. Miao<sup>7</sup> , M. Mikhasenko<sup>80</sup> , D.A. Milanese<sup>78,x</sup> , A. Minotti<sup>31,p</sup> , E. Minucci<sup>28</sup> , T. Miralles<sup>11</sup> , B. Mitreska<sup>64</sup> , D.S. Mitzel<sup>19</sup> , R. Mocanu<sup>43</sup> , A. Modak<sup>59</sup> , L. Moeser<sup>19</sup> , R.D. Moise<sup>17</sup> , E. F. Molina Cardenas<sup>88</sup> , T. Mombächer<sup>67</sup> , M. Monk<sup>57</sup> , T. Monnard<sup>51</sup> , S. Monteil<sup>11</sup> , A. Morcillo Gomez<sup>48</sup> , G. Morello<sup>28</sup> , M.J. Morello<sup>35,t</sup> , M.P. Morgenthaler<sup>22</sup> , A. Moro<sup>31,p</sup> , J. Moron<sup>40</sup> , W. Morren<sup>38</sup> , A.B. Morris<sup>82,50</sup> , A.G. Morris<sup>13</sup> , R. Mountain<sup>70</sup> , Z. Mu<sup>6</sup> , E. Muhammad<sup>58</sup> , F. Muheim<sup>60</sup> , M. Mulder<sup>38</sup> , K. Müller<sup>52</sup> , F. Muñoz-Rojas<sup>9</sup> , R. Murta<sup>63</sup> , V. Mytrochenko<sup>53</sup> , P. Naik<sup>62</sup> , T. Nakada<sup>51</sup> , R. Nandakumar<sup>59</sup> , T. Nanut<sup>50</sup> , G. Napoletano<sup>51</sup> , I. Nasteva<sup>3</sup> , M. Needham<sup>60</sup> , E. Nekrasova<sup>44</sup> , N. Neri<sup>30,o</sup> , S. Neubert<sup>18</sup> ,

N. Neufeld<sup>50</sup> , P. Neustroev<sup>44</sup>, J. Nicolini<sup>50</sup> , D. Nicotra<sup>84</sup> , E.M. Niel<sup>15</sup> , N. Nikitin<sup>44</sup> ,  
 L. Nisi<sup>19</sup> , Q. Niu<sup>75</sup> , B. K. Njoki<sup>50</sup> , P. Nogarolli<sup>3</sup> , P. Nogga<sup>18</sup> , C. Normand<sup>48</sup> ,  
 J. Novoa Fernandez<sup>48</sup> , G. Nowak<sup>67</sup> , C. Nunez<sup>88</sup> , H. N. Nur<sup>61</sup> ,  
 A. Oblakowska-Mucha<sup>40</sup> , V. Obraztsov<sup>44</sup> , T. Oeser<sup>17</sup> , A. Okhotnikov<sup>44</sup>,  
 O. Okhrimenko<sup>54</sup> , R. Oldeman<sup>32,l</sup> , F. Oliva<sup>60,50</sup> , E. Olivart Pino<sup>46</sup> , M. Olocco<sup>19</sup> ,  
 R.H. O'Neil<sup>50</sup> , J.S. Ordonez Soto<sup>11</sup> , D. Osthues<sup>19</sup> , J.M. Otalora Goicochea<sup>3</sup> ,  
 P. Owen<sup>52</sup> , A. Oyanguren<sup>49</sup> , O. Ozcelik<sup>50</sup> , F. Paciolla<sup>35,v</sup> , A. Padee<sup>42</sup> ,  
 K.O. Padeken<sup>18</sup> , B. Pagare<sup>48</sup> , T. Pajero<sup>50</sup> , A. Palano<sup>24</sup> , L. Palini<sup>30</sup> ,  
 M. Palutan<sup>28</sup> , C. Pan<sup>76</sup> , X. Pan<sup>4,d</sup> , S. Panebianco<sup>12</sup> , S. Paniskaki<sup>50,33</sup> ,  
 G. Panshin<sup>5</sup> , L. Paolucci<sup>64</sup> , A. Papanestis<sup>59</sup> , M. Pappagallo<sup>24,i</sup> , L.L. Pappalardo<sup>26</sup> ,  
 C. Pappenheimer<sup>67</sup> , C. Parkes<sup>64</sup> , D. Parmar<sup>80</sup> , G. Passaleva<sup>27</sup> , D. Passaro<sup>35,t</sup> ,  
 A. Pastore<sup>24</sup> , M. Patel<sup>63</sup> , J. Patoc<sup>65</sup> , C. Patrignani<sup>25,k</sup> , A. Paul<sup>70</sup> , C.J. Pawley<sup>84</sup> ,  
 A. Pellegrino<sup>38</sup> , J. Peng<sup>5,7</sup> , X. Peng<sup>75</sup>, M. Pepe Altarelli<sup>28</sup> , S. Perazzini<sup>25</sup> ,  
 D. Pereima<sup>44</sup> , H. Pereira Da Costa<sup>69</sup> , M. Pereira Martinez<sup>48</sup> , A. Pereiro Castro<sup>48</sup> , C.  
 Perez<sup>47</sup> , P. Perret<sup>11</sup> , A. Perrevoort<sup>83</sup> , A. Perro<sup>50</sup> , M.J. Peters<sup>67</sup> , K. Petridis<sup>56</sup> ,  
 A. Petrolini<sup>29,n</sup> , S. Pezzulo<sup>29,n</sup> , J. P. Pfaller<sup>67</sup> , H. Pham<sup>70</sup> , L. Pica<sup>35,t</sup> ,  
 M. Piccini<sup>34</sup> , L. Piccolo<sup>32</sup> , B. Pietrzyk<sup>10</sup> , G. Pietrzyk<sup>14</sup> , R. N. Pilato<sup>62</sup> ,  
 D. Pinci<sup>36</sup> , F. Pisani<sup>50</sup> , M. Pizzichemi<sup>31,p,50</sup> , V. M. Placinta<sup>43</sup> , M. Plo Casasus<sup>48</sup> ,  
 T. Poeschl<sup>50</sup> , F. Polci<sup>16</sup> , M. Poli Lener<sup>28</sup> , A. Poluektov<sup>13</sup> , N. Polukhina<sup>44</sup> ,  
 I. Polyakov<sup>64</sup> , E. Polycarpo<sup>3</sup> , S. Ponce<sup>50</sup> , D. Popov<sup>7,50</sup> , K. Popp<sup>19</sup> ,  
 S. Poslavskii<sup>44</sup> , K. Prasanth<sup>60</sup> , C. Prouve<sup>45</sup> , D. Provenzano<sup>32,l,50</sup> , V. Pugatch<sup>54</sup> , A.  
 Puicercus Gomez<sup>50</sup> , G. Punzi<sup>35,u</sup> , J.R. Pybus<sup>69</sup> , Q. Qian<sup>6</sup> , W. Qian<sup>7</sup> , N. Qin<sup>4,d</sup> ,  
 R. Quagliani<sup>50</sup> , R.I. Rabadan Trejo<sup>58</sup> , R. Racz<sup>82</sup> , J.H. Rademacker<sup>56</sup> , M. Rama<sup>35</sup> ,  
 M. Ramírez García<sup>88</sup> , V. Ramos De Oliveira<sup>71</sup> , M. Ramos Pernas<sup>58</sup> , M.S. Rangel<sup>3</sup> ,  
 F. Ratnikov<sup>44</sup> , G. Raven<sup>39</sup> , M. Rebollo De Miguel<sup>49</sup> , F. Redi<sup>30,j</sup> , J. Reich<sup>56</sup> ,  
 F. Reiss<sup>20</sup> , Z. Ren<sup>7</sup> , P.K. Resmi<sup>65</sup> , M. Ribalda Galvez<sup>46</sup> , R. Ribatti<sup>51</sup> ,  
 G. Ricart<sup>12</sup> , D. Riccardi<sup>35,t</sup> , S. Ricciardi<sup>59</sup> , K. Richardson<sup>66</sup> ,  
 M. Richardson-Slipper<sup>57</sup> , F. Riehn<sup>19</sup> , K. Rinnert<sup>62</sup> , P. Robbe<sup>14,50</sup> , G. Robertson<sup>61</sup> ,  
 E. Rodrigues<sup>62</sup> , A. Rodriguez Alvarez<sup>46</sup> , E. Rodriguez Fernandez<sup>48</sup> ,  
 J.A. Rodriguez Lopez<sup>78</sup> , E. Rodriguez Rodriguez<sup>50</sup> , J. Roensch<sup>19</sup> , A. Rogachev<sup>44</sup> ,  
 A. Rogovskiy<sup>59</sup> , D.L. Rolf<sup>19</sup> , P. Roloff<sup>50</sup> , V. Romanovskiy<sup>67</sup> , A. Romero Vidal<sup>48</sup> ,  
 G. Romolini<sup>26,50</sup> , F. Ronchetti<sup>51</sup> , T. Rong<sup>6</sup> , M. Rotondo<sup>28</sup> , S. R. Roy<sup>22</sup> ,  
 M.S. Rudolph<sup>70</sup> , M. Ruiz Diaz<sup>22</sup> , R.A. Ruiz Fernandez<sup>48</sup> , J. Ruiz Vidal<sup>84</sup> , J.  
 J. Saavedra-Arias<sup>9</sup> , J.J. Saborido Silva<sup>48</sup> , S. E. R. Sacha Emile R.<sup>50</sup> , N. Sagidova<sup>44</sup> ,  
 D. Sahoo<sup>81</sup> , N. Sahoo<sup>55</sup> , B. Saitta<sup>32</sup> , M. Salomoni<sup>31,50,p</sup> , I. Sanderswood<sup>49</sup> ,  
 R. Santacesaria<sup>36</sup> , C. Santamarina Rios<sup>48</sup> , M. Santimaria<sup>28</sup> , L. Santoro<sup>2</sup> ,  
 E. Santovetti<sup>37</sup> , A. Saputi<sup>26,50</sup> , D. Saranin<sup>44</sup> , A. Sarnatskiy<sup>83</sup> , G. Sarpis<sup>50</sup> ,  
 M. Sarpis<sup>82</sup> , C. Satriano<sup>36</sup> , A. Satta<sup>37</sup> , M. Saur<sup>75</sup> , D. Savrina<sup>44</sup> , H. Sazak<sup>17</sup> ,  
 F. Sborzacchi<sup>50,28</sup> , A. Scarabotto<sup>19</sup> , S. Schael<sup>17</sup> , S. Scherl<sup>62</sup> , M. Schiller<sup>22</sup> ,  
 H. Schindler<sup>50</sup> , M. Schmelling<sup>21</sup> , B. Schmidt<sup>50</sup> , N. Schmidt<sup>69</sup> , S. Schmitt<sup>66</sup> ,  
 H. Schmitz<sup>18</sup>, O. Schneider<sup>51</sup> , A. Schopper<sup>63</sup> , N. Schulte<sup>19</sup> , M.H. Schune<sup>14</sup> ,  
 G. Schwering<sup>17</sup> , B. Sciascia<sup>28</sup> , A. Sciuccati<sup>50</sup> , G. Scriven<sup>84</sup> , I. Segal<sup>80</sup> ,  
 S. Sellam<sup>48</sup> , A. Semennikov<sup>44</sup> , T. Senger<sup>52</sup> , M. Senghi Soares<sup>39</sup> , A. Sergi<sup>29,n</sup> ,  
 N. Serra<sup>52</sup> , L. Sestini<sup>27</sup> , A. Seuthe<sup>19</sup> , B. Sevilla Sanjuan<sup>47</sup> , Y. Shang<sup>6</sup> ,  
 D.M. Shangase<sup>88</sup> , M. Shapkin<sup>44</sup> , R. S. Sharma<sup>70</sup> , I. Shchemerov<sup>44</sup> , L. Shchutka<sup>51</sup> ,  
 T. Shears<sup>62</sup> , L. Shekhtman<sup>44</sup> , J. Shen<sup>6</sup>, Z. Shen<sup>38</sup> , S. Sheng<sup>51</sup> , V. Shevchenko<sup>44</sup> ,  
 B. Shi<sup>7</sup> , J. Shi<sup>57</sup> , Q. Shi<sup>7</sup> , W. S. Shi<sup>74</sup> , Y. Shimizu<sup>14</sup> , E. Shmanin<sup>25</sup> ,  
 R. Shorkin<sup>44</sup> , J.D. Shupperd<sup>70</sup> , R. Silva Coutinho<sup>2</sup> , G. Simi<sup>33,r</sup> , S. Simone<sup>24,i</sup> , M.  
 Singha<sup>81</sup> , I. Siral<sup>51</sup> , N. Skidmore<sup>58</sup> , T. Skwarnicki<sup>70</sup> , M.W. Slater<sup>55</sup> , E. Smith<sup>66</sup> ,  
 M. Smith<sup>63</sup> , L. Soares Lavra<sup>60</sup> , M.D. Sokoloff<sup>67</sup> , F.J.P. Soler<sup>61</sup> , A. Solomin<sup>56</sup> ,

A. Solovov<sup>44</sup> , K. Solovieva<sup>20</sup> , N. S. Sommerfeld<sup>18</sup> , R. Song<sup>1</sup> , Y. Song<sup>51</sup> ,  
 Y. Song<sup>4,d</sup> , Y. S. Song<sup>6</sup> , F.L. Souza De Almeida<sup>46</sup> , B. Souza De Paula<sup>3</sup> ,  
 K.M. Sowa<sup>40</sup> , E. Spadaro Norella<sup>29,n</sup> , E. Spedicato<sup>25</sup> , J.G. Speer<sup>19</sup> , P. Spradlin<sup>61</sup> ,  
 F. Stagni<sup>50</sup> , M. Stahl<sup>80</sup> , S. Stahl<sup>50</sup> , S. Stanislaus<sup>65</sup> , M. Stefaniak<sup>89</sup> ,  
 O. Steinkamp<sup>52</sup> , D. Strelalina<sup>44</sup> , Y. Su<sup>7</sup> , F. Suljik<sup>65</sup> , J. Sun<sup>32</sup> , J. Sun<sup>64</sup> ,  
 L. Sun<sup>76</sup> , D. Sundfeld<sup>2</sup> , W. Sutcliffe<sup>52</sup> , P. Svihra<sup>79</sup> , V. Svintozelskyi<sup>49</sup> ,  
 K. Swientek<sup>40</sup> , F. Swystun<sup>57</sup> , A. Szabelski<sup>42</sup> , T. Szumlak<sup>40</sup> , Y. Tan<sup>4</sup> , Y. Tang<sup>76</sup> ,  
 Y. T. Tang<sup>7</sup> , M.D. Tat<sup>22</sup> , J. A. Teijeiro Jimenez<sup>48</sup> , A. Terentev<sup>44</sup> , F. Terzuoli<sup>35,v</sup> ,  
 F. Teubert<sup>50</sup> , E. Thomas<sup>50</sup> , D.J.D. Thompson<sup>55</sup> , A. R. Thomson-Strong<sup>60</sup> ,  
 H. Tilquin<sup>63</sup> , V. Tisserand<sup>11</sup> , S. T'Jampens<sup>10</sup> , M. Tobin<sup>5,50</sup> , T. T. Todorov<sup>20</sup> ,  
 L. Tomassetti<sup>26,m</sup> , G. Tonani<sup>30</sup> , X. Tong<sup>6</sup> , T. Tork<sup>30</sup> , L. Toscano<sup>19</sup> , D.Y. Tou<sup>4,d</sup> ,  
 C. Trippi<sup>47</sup> , G. Tuci<sup>22</sup> , N. Tuning<sup>38</sup> , L.H. Uecker<sup>22</sup> , A. Ukleja<sup>40</sup> ,  
 D.J. Unverzagt<sup>22</sup> , A. Upadhyay<sup>50</sup> , B. Urbach<sup>60</sup> , A. Usachov<sup>38</sup> , A. Ustyuzhanin<sup>44</sup> ,  
 U. Uwer<sup>22</sup> , V. Vagnoni<sup>25,50</sup> , A. Vaitkevicius<sup>82</sup> , V. Valcarce Cadenas<sup>48</sup> ,  
 G. Valenti<sup>25</sup> , N. Valls Canudas<sup>50</sup> , J. van Eldik<sup>50</sup> , H. Van Hecke<sup>69</sup> ,  
 E. van Herwijnen<sup>63</sup> , C.B. Van Hulse<sup>48,y</sup> , R. Van Laak<sup>51</sup> , M. van Veghel<sup>84</sup> ,  
 G. Vasquez<sup>52</sup> , R. Vazquez Gomez<sup>46</sup> , P. Vazquez Regueiro<sup>48</sup> , C. Vázquez Sierra<sup>45</sup> ,  
 S. Vecchi<sup>26</sup> , J. Velilla Serna<sup>49</sup> , J.J. Velthuis<sup>56</sup> , M. Veltri<sup>27,w</sup> , A. Venkateswaran<sup>51</sup> ,  
 M. Verdoglia<sup>32</sup> , M. Vesterinen<sup>58</sup> , W. Vetens<sup>70</sup> , D. Vico Benet<sup>65</sup> , P.  
 Vidrier Villalba<sup>46</sup> , M. Vieites Diaz<sup>48</sup> , X. Vilasis-Cardona<sup>47</sup> , E. Vilella Figueras<sup>62</sup> ,  
 A. Villa<sup>25</sup> , P. Vincent<sup>16</sup> , B. Vivacqua<sup>3</sup> , F.C. Volle<sup>55</sup> , D. vom Bruch<sup>13</sup> ,  
 N. Voropaev<sup>44</sup> , K. Vos<sup>84</sup> , C. Vrahas<sup>60</sup> , J. Wagner<sup>19</sup> , J. Walsh<sup>35</sup> , E.J. Walton<sup>1</sup> ,  
 G. Wan<sup>6</sup> , A. Wang<sup>7</sup> , B. Wang<sup>5</sup> , C. Wang<sup>22</sup> , G. Wang<sup>8</sup> , H. Wang<sup>75</sup> ,  
 J. Wang<sup>7</sup> , J. Wang<sup>5</sup> , J. Wang<sup>4,d</sup> , J. Wang<sup>76</sup> , M. Wang<sup>50</sup> , N. W. Wang<sup>7</sup> ,  
 R. Wang<sup>56</sup> , X. Wang<sup>8</sup> , X. Wang<sup>74</sup> , X. W. Wang<sup>63</sup> , Y. Wang<sup>77</sup> , Y. Wang<sup>6</sup> , Y. H.  
 Wang<sup>75</sup> , Z. Wang<sup>14</sup> , Z. Wang<sup>30</sup> , J.A. Ward<sup>58,1</sup> , M. Waterlaet<sup>50</sup> , N.K. Watson<sup>55</sup> ,  
 D. Websdale<sup>63</sup> , Y. Wei<sup>6</sup> , Z. Weida<sup>7</sup> , J. Wendel<sup>45</sup> , B.D.C. Westhenry<sup>56</sup> ,  
 C. White<sup>57</sup> , M. Whitehead<sup>61</sup> , E. Whiter<sup>55</sup> , A.R. Wiederhold<sup>64</sup> , D. Wiedner<sup>19</sup> , M.  
 A. Wiegertjes<sup>38</sup> , C. Wild<sup>65</sup> , G. Wilkinson<sup>65,50</sup> , M.K. Wilkinson<sup>67</sup> , M. Williams<sup>66</sup> ,  
 M. J. Williams<sup>50</sup> , M.R.J. Williams<sup>60</sup> , R. Williams<sup>57</sup> , S. Williams<sup>56</sup> , Z. Williams<sup>56</sup> ,  
 F.F. Wilson<sup>59</sup> , M. Winn<sup>12</sup> , W. Wislicki<sup>42</sup> , M. Witek<sup>41</sup> , L. Witola<sup>19</sup> , T. Wolf<sup>22</sup> , E.  
 Wood<sup>57</sup> , G. Wormser<sup>14</sup> , S.A. Wotton<sup>57</sup> , H. Wu<sup>70</sup> , J. Wu<sup>8</sup> , X. Wu<sup>76</sup> , Y. Wu<sup>6,57</sup> ,  
 Z. Wu<sup>7</sup> , K. Wyllie<sup>50</sup> , S. Xian<sup>74</sup> , Z. Xiang<sup>5</sup> , Y. Xie<sup>8</sup> , T. X. Xing<sup>30</sup> , A. Xu<sup>35,t</sup> ,  
 L. Xu<sup>4,d</sup> , M. Xu<sup>50</sup> , Z. Xu<sup>50</sup> , Z. Xu<sup>7</sup> , Z. Xu<sup>5</sup> , S. Yadav<sup>26</sup> , K. Yang<sup>63</sup> ,  
 X. Yang<sup>6</sup> , Y. Yang<sup>7</sup> , Y. Yang<sup>81</sup> , Z. Yang<sup>6</sup> , V. Yeroshenko<sup>14</sup> , H. Yeung<sup>64</sup> ,  
 H. Yin<sup>8</sup> , X. Yin<sup>7</sup> , C. Y. Yu<sup>6</sup> , J. Yu<sup>73</sup> , X. Yuan<sup>5</sup> , Y. Yuan<sup>5,7</sup> , J.  
 A. Zamora Saa<sup>72</sup> , M. Zavertyaev<sup>21</sup> , M. Zdybal<sup>41</sup> , F. Zenesini<sup>25</sup> , C. Zeng<sup>5,7</sup> ,  
 M. Zeng<sup>4,d</sup> , C. Zhang<sup>6</sup> , D. Zhang<sup>8</sup> , J. Zhang<sup>7</sup> , L. Zhang<sup>4,d</sup> , R. Zhang<sup>8</sup> ,  
 S. Zhang<sup>65</sup> , S. L. Zhang<sup>73</sup> , Y. Zhang<sup>6</sup> , Y. Z. Zhang<sup>4,d</sup> , Z. Zhang<sup>4,d</sup> , Y. Zhao<sup>22</sup> ,  
 A. Zhelezov<sup>22</sup> , S. Z. Zheng<sup>6</sup> , X. Z. Zheng<sup>4,d</sup> , Y. Zheng<sup>7</sup> , T. Zhou<sup>6</sup> , X. Zhou<sup>8</sup> ,  
 Y. Zhou<sup>7</sup> , V. Zhovkovska<sup>58</sup> , L. Z. Zhu<sup>7</sup> , X. Zhu<sup>4,d</sup> , X. Zhu<sup>8</sup> , Y. Zhu<sup>17</sup> ,  
 V. Zhukov<sup>17</sup> , J. Zhuo<sup>49</sup> , D. Zuliani<sup>33,r</sup> , G. Zunica<sup>28</sup> .

<sup>1</sup>*School of Physics and Astronomy, Monash University, Melbourne, Australia*

<sup>2</sup>*Centro Brasileiro de Pesquisas Físicas (CBPF), Rio de Janeiro, Brazil*

<sup>3</sup>*Universidade Federal do Rio de Janeiro (UFRJ), Rio de Janeiro, Brazil*

<sup>4</sup>*Department of Engineering Physics, Tsinghua University, Beijing, China*

<sup>5</sup>*Institute Of High Energy Physics (IHEP), Beijing, China*

<sup>6</sup>*School of Physics State Key Laboratory of Nuclear Physics and Technology, Peking University, Beijing, China*

<sup>7</sup>*University of Chinese Academy of Sciences, Beijing, China*

- <sup>8</sup>*Institute of Particle Physics, Central China Normal University, Wuhan, Hubei, China*
- <sup>9</sup>*Consejo Nacional de Rectores (CONARE), San Jose, Costa Rica*
- <sup>10</sup>*Université Savoie Mont Blanc, CNRS, IN2P3-LAPP, Annecy, France*
- <sup>11</sup>*Université Clermont Auvergne, CNRS/IN2P3, LPC, Clermont-Ferrand, France*
- <sup>12</sup>*Université Paris-Saclay, Centre d'Etudes de Saclay (CEA), IRFU, Gif-Sur-Yvette, France*
- <sup>13</sup>*Aix Marseille Univ, CNRS/IN2P3, CPPM, Marseille, France*
- <sup>14</sup>*Université Paris-Saclay, CNRS/IN2P3, IJCLab, Orsay, France*
- <sup>15</sup>*Laboratoire Leprince-Ringuet, CNRS/IN2P3, Ecole Polytechnique, Institut Polytechnique de Paris, Palaiseau, France*
- <sup>16</sup>*Laboratoire de Physique Nucléaire et de Hautes Énergies (LPNHE), Sorbonne Université, CNRS/IN2P3, Paris, France*
- <sup>17</sup>*I. Physikalisches Institut, RWTH Aachen University, Aachen, Germany*
- <sup>18</sup>*Universität Bonn - Helmholtz-Institut für Strahlen und Kernphysik, Bonn, Germany*
- <sup>19</sup>*Fakultät Physik, Technische Universität Dortmund, Dortmund, Germany*
- <sup>20</sup>*Physikalisches Institut, Albert-Ludwigs-Universität Freiburg, Freiburg, Germany*
- <sup>21</sup>*Max-Planck-Institut für Kernphysik (MPIK), Heidelberg, Germany*
- <sup>22</sup>*Physikalisches Institut, Ruprecht-Karls-Universität Heidelberg, Heidelberg, Germany*
- <sup>23</sup>*School of Physics, University College Dublin, Dublin, Ireland*
- <sup>24</sup>*INFN Sezione di Bari, Bari, Italy*
- <sup>25</sup>*INFN Sezione di Bologna, Bologna, Italy*
- <sup>26</sup>*INFN Sezione di Ferrara, Ferrara, Italy*
- <sup>27</sup>*INFN Sezione di Firenze, Firenze, Italy*
- <sup>28</sup>*INFN Laboratori Nazionali di Frascati, Frascati, Italy*
- <sup>29</sup>*INFN Sezione di Genova, Genova, Italy*
- <sup>30</sup>*INFN Sezione di Milano, Milano, Italy*
- <sup>31</sup>*INFN Sezione di Milano-Bicocca, Milano, Italy*
- <sup>32</sup>*INFN Sezione di Cagliari, Monserrato, Italy*
- <sup>33</sup>*INFN Sezione di Padova, Padova, Italy*
- <sup>34</sup>*INFN Sezione di Perugia, Perugia, Italy*
- <sup>35</sup>*INFN Sezione di Pisa, Pisa, Italy*
- <sup>36</sup>*INFN Sezione di Roma La Sapienza, Roma, Italy*
- <sup>37</sup>*INFN Sezione di Roma Tor Vergata, Roma, Italy*
- <sup>38</sup>*Nikhef National Institute for Subatomic Physics, Amsterdam, Netherlands*
- <sup>39</sup>*Nikhef National Institute for Subatomic Physics and VU University Amsterdam, Amsterdam, Netherlands*
- <sup>40</sup>*AGH - University of Krakow, Faculty of Physics and Applied Computer Science, Kraków, Poland*
- <sup>41</sup>*Henryk Niewodniczanski Institute of Nuclear Physics Polish Academy of Sciences, Kraków, Poland*
- <sup>42</sup>*National Center for Nuclear Research (NCBJ), Warsaw, Poland*
- <sup>43</sup>*Horia Hulubei National Institute of Physics and Nuclear Engineering, Bucharest-Magurele, Romania*
- <sup>44</sup>*Authors affiliated with an institute formerly covered by a cooperation agreement with CERN.*
- <sup>45</sup>*Universidad de Coruña, A Coruña, Spain*
- <sup>46</sup>*ICCUB, Universitat de Barcelona, Barcelona, Spain*
- <sup>47</sup>*La Salle, Universitat Ramon Llull, Barcelona, Spain*
- <sup>48</sup>*Instituto Galego de Física de Altas Enerxías (IGFAE), Universidade de Santiago de Compostela, Santiago de Compostela, Spain*
- <sup>49</sup>*Instituto de Física Corpuscular, Centro Mixto Universidad de Valencia - CSIC, Valencia, Spain*
- <sup>50</sup>*European Organization for Nuclear Research (CERN), Geneva, Switzerland*
- <sup>51</sup>*Institute of Physics, Ecole Polytechnique Fédérale de Lausanne (EPFL), Lausanne, Switzerland*
- <sup>52</sup>*Physik-Institut, Universität Zürich, Zürich, Switzerland*
- <sup>53</sup>*NSC Kharkiv Institute of Physics and Technology (NSC KIPT), Kharkiv, Ukraine*
- <sup>54</sup>*Institute for Nuclear Research of the National Academy of Sciences (KINR), Kyiv, Ukraine*
- <sup>55</sup>*School of Physics and Astronomy, University of Birmingham, Birmingham, United Kingdom*
- <sup>56</sup>*H.H. Wills Physics Laboratory, University of Bristol, Bristol, United Kingdom*
- <sup>57</sup>*Cavendish Laboratory, University of Cambridge, Cambridge, United Kingdom*
- <sup>58</sup>*Department of Physics, University of Warwick, Coventry, United Kingdom*
- <sup>59</sup>*STFC Rutherford Appleton Laboratory, Didcot, United Kingdom*

- <sup>60</sup> *School of Physics and Astronomy, University of Edinburgh, Edinburgh, United Kingdom*
- <sup>61</sup> *School of Physics and Astronomy, University of Glasgow, Glasgow, United Kingdom*
- <sup>62</sup> *Oliver Lodge Laboratory, University of Liverpool, Liverpool, United Kingdom*
- <sup>63</sup> *Imperial College London, London, United Kingdom*
- <sup>64</sup> *Department of Physics and Astronomy, University of Manchester, Manchester, United Kingdom*
- <sup>65</sup> *Department of Physics, University of Oxford, Oxford, United Kingdom*
- <sup>66</sup> *Massachusetts Institute of Technology, Cambridge, MA, United States*
- <sup>67</sup> *University of Cincinnati, Cincinnati, OH, United States*
- <sup>68</sup> *University of Maryland, College Park, MD, United States*
- <sup>69</sup> *Los Alamos National Laboratory (LANL), Los Alamos, NM, United States*
- <sup>70</sup> *Syracuse University, Syracuse, NY, United States*
- <sup>71</sup> *Pontifícia Universidade Católica do Rio de Janeiro (PUC-Rio), Rio de Janeiro, Brazil, associated to <sup>3</sup>*
- <sup>72</sup> *Universidad Andres Bello, Santiago, Chile, associated to <sup>52</sup>*
- <sup>73</sup> *School of Physics and Electronics, Hunan University, Changsha City, China, associated to <sup>8</sup>*
- <sup>74</sup> *State Key Laboratory of Nuclear Physics and Technology, South China Normal University, Guangzhou, China, associated to <sup>4</sup>*
- <sup>75</sup> *Lanzhou University, Lanzhou, China, associated to <sup>5</sup>*
- <sup>76</sup> *School of Physics and Technology, Wuhan University, Wuhan, China, associated to <sup>4</sup>*
- <sup>77</sup> *Henan Normal University, Xinxiang, China, associated to <sup>8</sup>*
- <sup>78</sup> *Departamento de Física , Universidad Nacional de Colombia, Bogota, Colombia, associated to <sup>16</sup>*
- <sup>79</sup> *Institute of Physics of the Czech Academy of Sciences, Prague, Czech Republic, associated to <sup>64</sup>*
- <sup>80</sup> *Ruhr Universitaet Bochum, Fakultae f. Physik und Astronomie, Bochum, Germany, associated to <sup>19</sup>*
- <sup>81</sup> *Eotvos Lorand University, Budapest, Hungary, associated to <sup>50</sup>*
- <sup>82</sup> *Faculty of Physics, Vilnius University, Vilnius, Lithuania, associated to <sup>20</sup>*
- <sup>83</sup> *Van Swinderen Institute, University of Groningen, Groningen, Netherlands, associated to <sup>38</sup>*
- <sup>84</sup> *Universiteit Maastricht, Maastricht, Netherlands, associated to <sup>38</sup>*
- <sup>85</sup> *Tadeusz Kosciuszko Cracow University of Technology, Cracow, Poland, associated to <sup>41</sup>*
- <sup>86</sup> *Department of Physics and Astronomy, Uppsala University, Uppsala, Sweden, associated to <sup>61</sup>*
- <sup>87</sup> *Taras Schevchenko University of Kyiv, Faculty of Physics, Kyiv, Ukraine, associated to <sup>14</sup>*
- <sup>88</sup> *University of Michigan, Ann Arbor, MI, United States, associated to <sup>70</sup>*
- <sup>89</sup> *Ohio State University, Columbus, United States, associated to <sup>69</sup>*

<sup>a</sup> *Universidade Estadual de Campinas (UNICAMP), Campinas, Brazil*

<sup>b</sup> *Centro Federal de Educação Tecnológica Celso Suckow da Fonseca, Rio De Janeiro, Brazil*

<sup>c</sup> *Department of Physics and Astronomy, University of Victoria, Victoria, Canada*

<sup>d</sup> *Center for High Energy Physics, Tsinghua University, Beijing, China*

<sup>e</sup> *Hangzhou Institute for Advanced Study, UCAS, Hangzhou, China*

<sup>f</sup> *LIP6, Sorbonne Université, Paris, France*

<sup>g</sup> *Lamarr Institute for Machine Learning and Artificial Intelligence, Dortmund, Germany*

<sup>h</sup> *Universidad Nacional Autónoma de Honduras, Tegucigalpa, Honduras*

<sup>i</sup> *Università di Bari, Bari, Italy*

<sup>j</sup> *Università di Bergamo, Bergamo, Italy*

<sup>k</sup> *Università di Bologna, Bologna, Italy*

<sup>l</sup> *Università di Cagliari, Cagliari, Italy*

<sup>m</sup> *Università di Ferrara, Ferrara, Italy*

<sup>n</sup> *Università di Genova, Genova, Italy*

<sup>o</sup> *Università degli Studi di Milano, Milano, Italy*

<sup>p</sup> *Università degli Studi di Milano-Bicocca, Milano, Italy*

<sup>q</sup> *Università di Modena e Reggio Emilia, Modena, Italy*

<sup>r</sup> *Università di Padova, Padova, Italy*

<sup>s</sup> *Università di Perugia, Perugia, Italy*

<sup>t</sup> *Scuola Normale Superiore, Pisa, Italy*

<sup>u</sup> *Università di Pisa, Pisa, Italy*

<sup>v</sup> *Università di Siena, Siena, Italy*

<sup>w</sup> *Università di Urbino, Urbino, Italy*

<sup>x</sup> *Universidad de Ingeniería y Tecnología (UTEC), Lima, Peru*

<sup>y</sup> *Universidad de Alcalá, Alcalá de Henares , Spain*

† *Deceased*